

CHLOROPHYLL-A CONCENTRATIONS AFFECTED BY FRESHWATER INFLOW  
AND CLIMATE CONDITIONS IN GALVESTON BAY, TEXAS

A Thesis

by

XIAO SHEN

Submitted to the Office of Graduate and Professional Studies of  
Texas A&M University  
in partial fulfillment of the requirements for the degree of

MASTER OF SCIENCE

Chair of Committee,	Huilin Gao
Committee Members,	Daniel Roelke
	Jacqueline Ann Aitkenhead-Peterson
Intercollegiate Faculty Chair,	R. Karthikeyan

December 2017

Major Subject: Water Management & Hydrological Science

Copyright 2017 Xiao Shen

## ABSTRACT

As transition zones between river and ocean, estuaries face increasing pressure on their ecosystem health due to changes of freshwater quantity and quality – especially under the impacts of population growth, land use/land cover change, and climate change. Located southeast of Houston, Galveston Bay is of particular social and economic importance for the State of Texas. Its freshwater inflow primarily arises from the San Jacinto River and the Trinity River. While it is well recognized that Chlorophyll a (chl<sub>a</sub>) concentration – an indicator of ecosystem health – is closely linked to river inflows and other environmental factors, no quantitative relationships have been established. The objectives of this study are to identify the spatial-temporal variations of chl<sub>a</sub>, and to investigate the impacts of freshwater inflow and climatic factors on chl<sub>a</sub> variability – so that prediction models can be developed for chl<sub>a</sub> forecasting in Galveston Bay.

A 10-year validated remote sensing chl<sub>a</sub> dataset is used in this study. Spatially, there are two spots with low chl<sub>a</sub> concentration compared with other places, locations close to the river mouths and the area of the bay where Houston Ship Channel located. Temporally, chl<sub>a</sub> tends to be higher in wet years than in dry years. Similarly, the seasonal fluctuations of chl<sub>a</sub> are more significant during the wet months (from February to May) than the dry months (especially from August to December). Chl<sub>a</sub> concentrations in different segments of Galveston Bay are determined by different factors during different seasons. Discharge from the Trinity River is the main driver of chl<sub>a</sub> in JFM (January, February, March), AMJ (April, May, June) and JAS (July, August, September) in all

segments, except West Bay (where the chl<sub>a</sub> concentration is mainly determined by climatological variations). Also, water temperature plays a significant role in regulating chl<sub>a</sub>, especially in JFM. Based on these analyses, a chl<sub>a</sub> prediction model is developed and tested. Despite its limitations, this empirical model offers seasonal forecasts of chl<sub>a</sub> which could support decision making in Galveston Bay.

## ACKNOWLEDGEMENTS

I would like to thank my committee chair, Dr. Gao, and my committee members, Dr. Peterson and Dr. Roelke, for their guidance and support during my research endeavors. I also wish to extend special thanks to my peers in Dr. Gao's research group for their encouragement and help throughout my graduate study.

To my parents, and to my friends, thank you for your strong encouragement and support throughout these two years.

## CONTRIBUTORS AND FUNDING SOURCES

This work was supervised by a thesis committee consisting of Dr. Huilin Gao of the Department of Civil Engineering, Dr. Jacqueline Ann Aitkenhead-Peterson of the Department of Soil and Crop Sciences, and Dr. Daniel Roelke of the Department of Wildlife and Fisheries Sciences.

The Chlorophyll-a (chl<sub>a</sub>) in-situ data were provided by Dr. Antonietta Quigg from Texas A&M University, Galveston (TAMUG). The curvilinear relationship between the gauge height and discharge rate at Lake Houston (29.96° N, 95.16°W) was provided by Dr. Kyeong Park's group at TAMUG. Water temperature data were provided by Texas Water Development Board (TWDB). The remotely sensed chl<sub>a</sub> concentrations were generated by Dr. Shuai Zhang in Dr. Huilin Gao's research group.

This work was funded by the Texas Coastal Management Program (CMP-16-055), as well as the National Science Foundation – CAREER Grant (CBET 1454297). The contents of this thesis are solely the responsibility of the author and do not necessarily represent the official views of Texas A&M University, Water Management & Hydrological Science, nor the National Science Foundation.

## TABLE OF CONTENTS

	Page
ABSTRACT .....	ii
ACKNOWLEDGEMENTS .....	iv
CONTRIBUTORS AND FUNDING SOURCES .....	v
TABLE OF CONTENTS .....	vi
LIST OF FIGURES .....	viii
LIST OF TABLES .....	x
1. INTRODUCTION .....	1
1.1 Chlorophyll a and Environment Factors .....	1
1.2 Chla Monitoring and Remote Sensing .....	4
1.3 Chla Prediction .....	5
1.4 Chla Conditions in Galveston Bay .....	6
1.5 Research Objectives .....	7
2. STUDY AREA .....	9
3. DATA & METHODS .....	12
3.1 Data Sources .....	12
3.2 Methods .....	15
3.2.1 Segments division .....	15
3.2.2 Chla spatiotemporal analysis .....	16
3.2.3 Chla driving factors analysis .....	17
3.2.4 Constructing a chla prediction model .....	18
4. RESULTS .....	21
4.1 Spatial and Temporal Variability of Chla .....	21
4.1.1 Spatial distribution of chla .....	21
4.1.2 Inter-annual variability of chla .....	25
4.1.3 Monthly variability of chla .....	26
4.2 Chla Driving Factors: Freshwater Inflow and Climate Conditions .....	29
4.2.1 Freshwater inflow .....	30

4.2.2 Climate conditions .....	32
4.2.3 Seasonal correlation between chl <sub>a</sub> and environmental factors .....	33
4.3 Chl <sub>a</sub> Prediction Model .....	46
4.3.1 Trinity Bay and San Jacinto Bay .....	47
4.3.2 East Bay and Lower Bay.....	52
4.3.3 West Bay .....	55
4.3.4 Relationship between air temperature and water temperature .....	57
5. DISCUSSION .....	59
6. CONCLUSIONS .....	62
REFERENCES .....	65
APPENDIX A .....	72
APPENDIX B .....	74

## LIST OF FIGURES

	Page
Figure 2-1. The map of Galveston Bay in Texas .....	9
Figure 3-1. MERIS chla data calibrated and validated against in-situ data.....	13
Figure 3-2. Monthly discharge from the Trinity River and the San Jacinto River.....	14
Figure 3-3. The segments are divided based on hydrodynamic simulation results from the Environmental Fluid Dynamics Code.....	16
Figure 3-4. Calculation of relative weights for a regression model with three predictors, k=3 .....	18
Figure 4-1. Annual chla spatial distributions.....	23
Figure 4-2. Monthly chla spatial distributions.....	24
Figure 4-3. Time series of chla and discharge over May 2002 to December 2011 .....	28
Figure 4-4. The chla correlations among five segments.....	29
Figure 4-5. Time series of monthly discharge and chla concentration in (a) Trinity Bay and (b) San Jacinto Bay.....	31
Figure 4-6. Time series of (a) MEI; (b) water temperature anomalies; (c) chla anomalies from Trinity Bay; (d) chla anomalies from San Jacinto Bay.....	33
Figure 4-7. The monthly average correlation among $C_T$ , $C_S$ , T, MEI, $Q_T$ and $Q_S$ in (a) JFM; (b) AMJ; (c) JAS and (d) OND .....	36
Figure 4-8. Relative Importance of Predictor Variables in (a) Trinity Bay; (b) San Jacinto Bay.....	38
Figure 4-9. Relative Importance of Predictor Variables in (a) East Bay and (b) Lower Bay.....	39
Figure 4-10. Relative Importance of Predictor Variables in West Bay .....	40
Figure 4-11. The monthly average correlation among $C_E$ , $C_L$ , T, MEI, $Q_T$ and $Q_S$ in (a) JFM; (b) AMJ; (c) JAS and (d) OND.....	42



Figure 4-12. The monthly average correlation among $C_w$ , T, MEI, $Q_T$ and $Q_S$ in (a) JFM; (b) AMJ; (c) JAS and (d) OND. ....	44
Figure 4-13. Model prediction results in (a) Trinity Bay; (b) San Jacinto Bay; (c) the whole northern segment.....	51
Figure 4-14. Model prediction results in (a) East Bay; (b) Lower Bay .....	54
Figure 4-15. Model prediction results in West Bay .....	57
Figure 4-16. Linear regression relationship between air temperature and water temperature .....	58
Figure A-1 Water temperature monitoring station in Galveston Bay from Texas Water Development Board .....	72
Figure A-2 (a) Monthly water temperature time series from May 2002 to December 2012 (b) The water temperature differences among three monitoring station from 2009 to 2011 .....	72
Figure B-1 Comparison between prediction and observation chla in (a) Trinity Bay, (b) San Jacinto Bay and (c) Northern Segments average.....	74
Figure B-2 Comparison between prediction and observation chla in (a) East Bay, (b) Lower Bay and (c) West Bay.....	75

## LIST OF TABLES

	Page
Table 4-1. Significantly driving factors of chl <sub>a</sub> in each seasonal group ( $p < 0.01$ ). .....	41
Table 4-2. Prediction models developed in (a) Trinity Bay; (b) San Jacinto Bay; (c) Trinity Bay and San Jacinto Bay combined. ....	48
Table 4-3. Prediction model tested over Trinity Bay and San Jacinto Bay .....	50
Table 4-4. Prediction models developed in (a) East Bay; (b) Lower Bay .....	52
Table 4-5. Prediction model tested over East Bay and Lower Bay .....	54
Table 4-6. Prediction models developed in West Bay .....	55
Table 4-7. Prediction equation tested over West Bay .....	56

## 1. INTRODUCTION

### 1.1 Chlorophyll a and Environment Factors

Linking rivers with ocean environments, estuaries play an important role in aquatic ecosystem functions and service. However, many U.S. estuaries are threatened by various environmental problems, such as water quality degradation, eutrophication, and fish resources decline. A study by Bricker *et al.* (2008) showed that around 84 out of 139 U.S. coastal areas have experienced eutrophication. With regards to water quality monitoring, an abnormally high chlorophyll a (chl<sub>a</sub>) concentration is usually considered as a reliable indicator of eutrophication. The spatial and temporal distributions of chl<sub>a</sub> can be greatly influenced by freshwater inflow, circulation, salinity, sediment loading, nutrients loading, and water temperature (Harding 1994). In addition, the seasonal-to-interannual variabilities of coastal chl<sub>a</sub> are also indirectly affected by anthropogenic influences (such as urbanization, agriculture, and population development) and climatic influences (Harding *et al.* 2016).

By transporting nutrients and sediments—as well as by altering estuary circulations – freshwater inflow plays a key role in algae growth, which significantly affects chl<sub>a</sub> concentration levels. Especially with the ongoing population growth, extensive urbanization, and increased wastewater discharge that many areas are experiencing – combined with climate change – both the timing and the magnitude of freshwater inflows have become more sensitive and capricious (Cloern *et al.* 2001;

Roberts and Prince 2010; Camacho *et al.* 2015). By disturbing aquatic systems, phytoplankton community compositions and diversity, biomass and chl<sub>a</sub> concentration levels will be influenced by inflow events (Buyukates and Roelke 2004). In particular, freshwater inflow can impact phytoplankton biomass and chl<sub>a</sub> concentration indirectly, by affecting light availability, nutrient loading, flushing rate, stratification, and turbidity. A number of studies have investigated the impacts of freshwater inflow on chl<sub>a</sub> concentrations in coastal areas. For instance, studies using observational data over sixty years (1950 – 2010) in the Chesapeake Bay found that wet years resulted in large inflows and high chl<sub>a</sub> concentrations, while dry years led to small inflows and low chl<sub>a</sub> levels in the bay (Harding 2016). The research result from aircraft remote sensing of ocean color also confirmed the view reported nearly 30 years ago that magnitude of freshwater flows explained the inter-annual variability of phytoplankton biomass (Malone *et al.* 1988; Miller and Harding 2007). In the San Francisco Bay, an analysis of in-situ data by Cloern (1991) indicated a strong connection between the magnitude of annual spring algal blooms (during March – May) and the magnitude of the wet season (January through April) freshwater inflows from the Susquehanna River. In the Tampa Bay, Florida, the positive correlation between annual mean discharge and chl<sub>a</sub> was revealed as well based on the long-term observation from satellites (Le *et al.* 2013). In the Perdido Bay, Florida, it was found that large inflows could promote algae growth by reducing the anoxia and hypoxia conditions in the bay (Xia and Jiang 2015). In other international estuaries, similar positive correlations were identified – including in the Guadalquivir Estuary in Spain (Drake *et al.* 2002), the Loire River Estuary in France (Meybeck *et al.* 1988), and the Kasouga Estuary

in South Africa (Froneman 2002). Although most research results show that chl<sub>a</sub> often co-varies (usually positive correlations) with freshwater inflow, still for different systems, their relationships are usually diverse due to the different characteristics, such as circulation, residence time and tides (Miller and Harding 2007).

The seasonal and inter-annual variability of chl<sub>a</sub> concentrations in estuary regions are also strongly influenced by climatic variability (Miller and Harding 2007; Stenseth *et al.* 2002), which also affects freshwater inflow. Climate conditions can be represented by climatic indicators, such as water temperature and the El Niño-Southern Oscillation (ENSO) (Chavez *et al.* 1999; Cloern *et al.* 2011). They can influence estuaries' ecosystems strongly by affecting biological processes. For example, water temperature can affect biomass accumulation by changing the nutrient stratification and the algae grazing process. Similarly, because ENSO can alter the surface water temperature, the nutrient upwelling process, and the carbon dioxide storage in the water, the chl<sub>a</sub> concentration will be affected as well. In Tampa Bay, Florida, Le *et al.* (2013) found that a significant positive correlation existed between monthly mean chl<sub>a</sub> anomalies and the monthly Multivariate El Niño/Southern Oscillation Index (MEI), which indicated El Niño phenomenon associated with higher chl<sub>a</sub>. However, in the Equatorial Pacific Ocean, the El Niño phenomenon was found to be related to low chl<sub>a</sub> concentration levels (Chavez *et al.* 1999). These two different research results suggest that correlations between ENSO and phytoplankton biomass vary according to location and the different characteristics of the waterbodies. In the Chesapeake Bay, Miller and Harding (2007) found that when the winter is warmer and wetter than usual, the bloom in the following spring tends to be

greater in magnitude. Long-term (30+ years) research in this region also showed the lower chl<sub>a</sub> concentration in climatic-induced dry years compared with oppositely wet years (Harding *et al.* 2016). Research performed in the Buzzards Bay, Massachusetts, suggested that the increased temperature might worsen the degradation of the coastal system (Rheuban *et al.* 2016). In shallow waterbodies, such as in the Saginaw Bay and the Green Bay, Michigan, algal blooms could be exacerbated by warmer water temperature (Korosov *et al.* 2015). Thus, it is necessary to explore the combined influence of freshwater inflows and climatic conditions on plankton biomass levels in estuary regions.

## 1.2 Chl<sub>a</sub> Monitoring and Remote Sensing

Traditionally, chl<sub>a</sub> is monitored by field sampling. The measuring methods recommended by U.S. Environmental Protection Agency (EPA) include spectrophotometric method, the fluorometric method, and the high-performance liquid chromatography (HPLC) method (Dos *et al.* 2003). However, due to the cost and complexity involved in the data collection and processing (when using field sampling), the number of in-situ chl<sub>a</sub> measurements is often limited in time and space. Without long-term, continuous chl<sub>a</sub> observations, our capability of understanding and quantifying the impacts of inflow and climatic conditions on chl<sub>a</sub> variations is greatly hampered.

Satellite remote sensing has a number of advantages for monitoring chl<sub>a</sub> consistently with good spatial and temporal coverage at a high resolution (Sathyendranath *et al.* 2004). The main challenge in remote sensing of coastal chl<sub>a</sub> concentrations is the

reflectance noise associated with the atmosphere, other water quality components (such as the colored dissolved organic matters – CDOM, inorganic particles, and suspended sediment) and the reflection from shallow bottoms (Harding *et al.* 2005; Le *et al.* 2013). The chl<sub>a</sub> remote sensing algorithms are typically empirical (using various band combinations) and are validated against in-situ data (Liu *et al.* 2015; Le *et al.* 2016). The remotely sensed chl<sub>a</sub> datasets have been used to explore the environmental impacts on the estuary ecosystems in the Tampa Bay, the Chesapeake Bay, the Pensacola Bay, and other coastal areas over a long-term period (Le *et al.* 2013; Miller and Harding 2007; Han *et al.* 2005). As the technology continues to improve, remote sensing will provide even more opportunities for monitoring estuary eco-systems in the future.

### 1.3 Chl<sub>a</sub> Prediction

A chl<sub>a</sub> prediction model can be used to predict water quality deterioration in advance to mitigate point or non-point pollution sources, and to manage ecological health in estuaries. Generally, there are two types of methods used for chl<sub>a</sub> prediction: Mechanism-Driven models (MDMs), and Data-Driven approaches (DDAs) (Jiang *et al.* 2011).

MDMs are based on mechanisms of physical, chemical, and biological dynamics and interactions. They require a large amount of monitoring data (time series of hydrological, climatic and water quality indicators, etc.) and many environmental parameters, such as water quality parameters, hydrodynamic parameters, salinity and

temperature, etc. Thus, this method is less applicable for estuary management, especially for regions with limited sampling infrastructure (and also are often lacking in personnel with the necessary scientific background).

However, DDAs – such as multi-variable regression, neural network, and Artificial Neural Network – are based on statistics and are much easier to apply (due to less field sampling data requirements, as compared with MDMs). Therefore, the DDAs method is used in this study.

#### 1.4 Chla Conditions in Galveston Bay

As one of the seven major estuaries in Texas, Galveston Bay has significant ecological, economic and recreational values. Several studies have documented the chla variability and hydroclimatic influence on Galveston Bay. The alteration of upstream inflows (e.g., magnitude, timing and frequency) might exert a profound effect on ecological processes and corresponding ecosystem services in this region (Roelke *et al.* 2013; Dorado *et al.* 2015). By analyzing in-situ observations collected in two years (2005-2006), Roelke *et al.* (2013) found that the effects of freshwater inflows on chla varied in different sub-regions of Galveston Bay.

Although there has been lots of qualitative analysis (and explanations) presented about the relationships between the aforementioned environmental variables and chla concentrations in coastal regions, quantitative relationships have yet to be established. This especially hampers chla predictions, which are essential for supporting decision-



making. The limitations are primarily attributed to two causes: the lack of a reliable long-term chl<sub>a</sub> records in most estuary regions, and the lack of comprehensive analysis on those records that do exist. For instance, the joint impact of climatic conditions and freshwater inflows on chl<sub>a</sub> in Galveston Bay has never been thoroughly investigated. Thus, it is necessary to conduct a systemic study to establish a comprehensive understanding of the influence of different hydrological and climatic conditions on phytoplankton biomass dynamics over Galveston Bay area. To achieve this, long-term chl<sub>a</sub> observations from remote sensing will be leveraged.

### 1.5 Research Objectives

The objectives of this study are to identify the spatial-temporal variations of chl<sub>a</sub>, and to investigate the impacts of freshwater inflow and climatic factors on chl<sub>a</sub> variability – so that prediction models can be developed for chl<sub>a</sub> forecasting in Galveston Bay. To achieve these objectives, the spatial and temporal variabilities of chl<sub>a</sub> over a long-term (from May 2002 to December 2011) are first examined based on a remotely sensed dataset. Then, the effects of freshwater inflows and climate conditions on chl<sub>a</sub> concentration (both separately and jointly) are evaluated. Last, a chl<sub>a</sub> prediction model is established for supporting future ecological management in Galveston Bay. Specifically, the following questions are answered:

- (1) How does chl<sub>a</sub> concentration vary temporally and spatially in Galveston Bay?

(2) What are the roles of freshwater inflow and climatological factors in driving chla variations in Galveston Bay?

(3) Can we develop a robust empirical model for chla forecasting in Galveston Bay?

## 2. STUDY AREA

Galveston Bay (Figure 2-1), also referred to as the Trinity-San Jacinto Estuary, is located along the upper coast of Texas and is connected to the Gulf of Mexico. It is the seventh largest estuary in the U.S., bordering the fourth largest city and fifth largest metropolitan area by population in the nation. Due to these factors and others, it is home to a substantial industrial and maritime center. There are two major watersheds providing inflow into this estuary: the Trinity Basin and the San Jacinto Basin. These basins are home to two of the largest cities in the U.S. – Houston and Dallas – and include 60% of the major facilities in Texas (Ornolfsdottir *et al.* 2004). Half of the population in Texas currently lives within those two watersheds (Galveston Bay Report Card 2015).

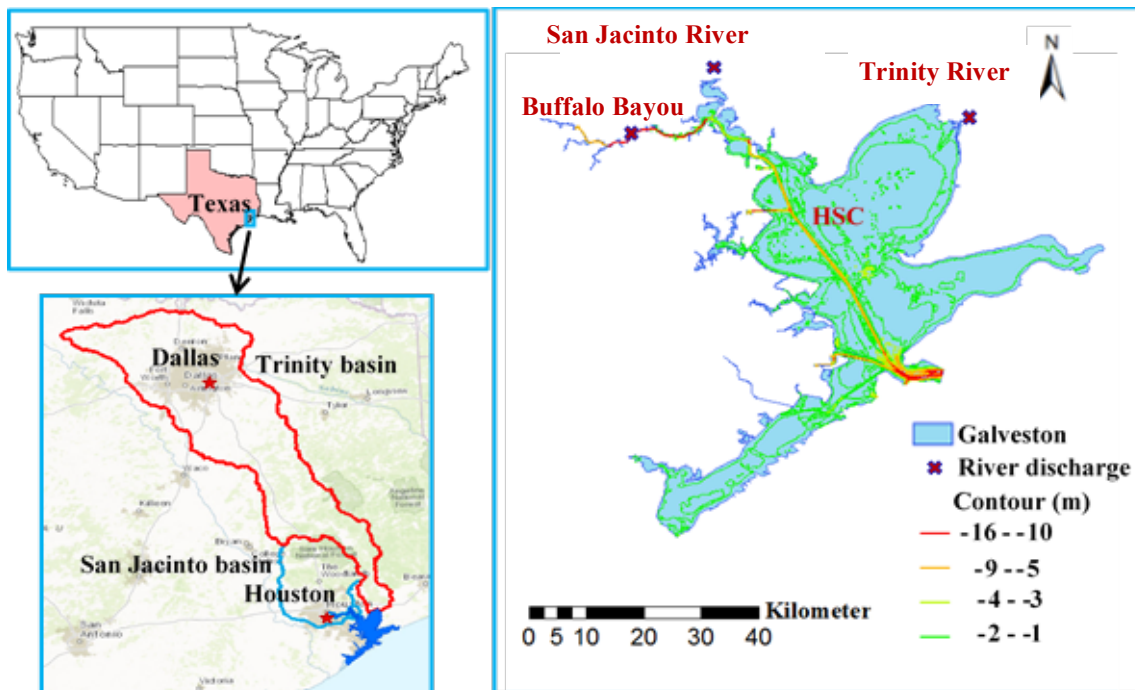


**Figure 2-1.** The map of Galveston Bay in Texas.

Galveston Bay covers an area of 1360 km<sup>2</sup> and has an average depth of 2 – 3 m. There is a man-made channel – the Houston Shipping Channel (HSC) – with a depth of 15 m that extends from the San Jacinto River in the northern part of the bay to the main Gulf entrance. Many areas surrounding Galveston Bay are highly urbanized and industrialized, which bring a significant amount of anthropogenic waste water input into the bay. Armstrong and Ward (1993) reported that about 30% – 60% of waste water in Texas is received by Galveston Bay. Freshwater inflows are primarily from two major rivers: the Trinity River and the San Jacinto River. Other smaller discharging rivers include Buffalo Bayou, Whiteoak Bayou, Brays Bayou, Huntington Bayou, Sims Bayou, and Greens Bayou. Historically, the San Jacinto River and the Trinity River contribute about 28% and 54% of total freshwater inflow, respectively (Roelke *et al.* 2013). According to the U.S. Geological Survey (USGS) data from 2002 to 2012, the average discharge from the Trinity River and the San Jacinto River are 211.2 m<sup>3</sup>/s and 67.7 m<sup>3</sup>/s, respectively. In such a shallow bay, freshwater inflows are an important mechanism for water mixing. The nutrients loading input into Galveston Bay is very large, estimated to be 8.4 million kg/year of nitrogen and 4.0 million kg/year of phosphorus (Armstrong and Ward 1993). However, the system has low to moderate chl<sub>a</sub> concentrations (2 – 20 µg/L) (Örnólfsson *et al.* 2004; Buskey and Schmidt 1992), with an average concentration of 12.8 µg/L (based on the field monitoring data from 2008 to 2015 provided by Dr. Antonietta Quigg).

In addition, Galveston Bay is located in a humid subtropical area of Texas, which is near the border of a semi-arid climate zone, making it much more vulnerable to extreme

hydrological events and climate conditions (e.g. drought and flood). The temperature range is roughly 4°C (winter) to 32 °C (summer), and the annual rainfall is usually over 1000 mm. Heat from the deserts of Mexico and moisture from the Gulf of Mexico are brought into this area by prevailing winds from the south and southeast. At the same time, it is regularly impacted by tropical storms and hurricanes (especially during fall seasons) (Guannel *et al.* 2014). On September 12, 2008, Hurricane Ike arrived on the south of Galveston, causing the whole coastal area of Galveston Bay to be inundated by saltwater.

### 3. DATA & METHODS

#### 3.1 Data Sources

Datasets used in this thesis include the remotely sensed chl<sub>a</sub> concentrations in Galveston Bay, the observed discharge data from both the Trinity River and the San Jacinto River, the water temperature, and the MEI. The period of data coverage is from May 22, 2002 to December 31, 2011 (roughly 10 years in total).

The remotely sensed Chl<sub>a</sub> concentrations were estimated by the MEdium Resolution Imaging Spectrometer (MERIS) (Zhang *et al.* 2017), which was one of the main instruments on board of the European Space Agency (ESA)'s Envisat platform. The spatial resolution of MERIS is 260m × 300m and temporal resolution is 3-day. The Level 1b (L1b) band 7 (664 nm), band 8 (681 nm), and band 9 (708 nm) reflectance data are used to calculate Fluorescence Line Height (FLH) in Galveston Bay. The Second Simulation of the Satellite Signal in the Solar Spectrum model (6S V2.1) is adopted to correct atmospheric effects. Chl<sub>a</sub> in situ data is monitored from surface (0 – 0.3m) water samples collected from 6 – 41 stations around the Bay. The remotely sensed FLH from MERIS is calibrated and validated against in-situ data over the corresponding sampling locations, and a regression equation applicable to the entire Galveston Bay is generated, which is shown in Figure 3-1 (Zhang *et al.* 2017). Then the chl<sub>a</sub> product is developed by applying the empirical equations to each MERIS image from 2002 to 2011. The 3-day

products are further averaged to monthly to reduce noise associated with MERIS reflectance.

Freshwater inflow (Figure 3-2) from the Trinity River is obtained from the US Geological Survey gauge station at Romayor (station #08066500). Inflow from the San Jacinto River is inferred as the total discharge of the Buffalo Bayou in Houston (station #08074500), the Buffalo Bayou at Houston (station #08074000) and the Lake Houston discharge (station #08072050). Among the three, the discharge from Lake Houston is calculated based on the curvilinear relationship between gauge height and discharge (personal communication, Dr. Kyeong Park's group, TAMUG).

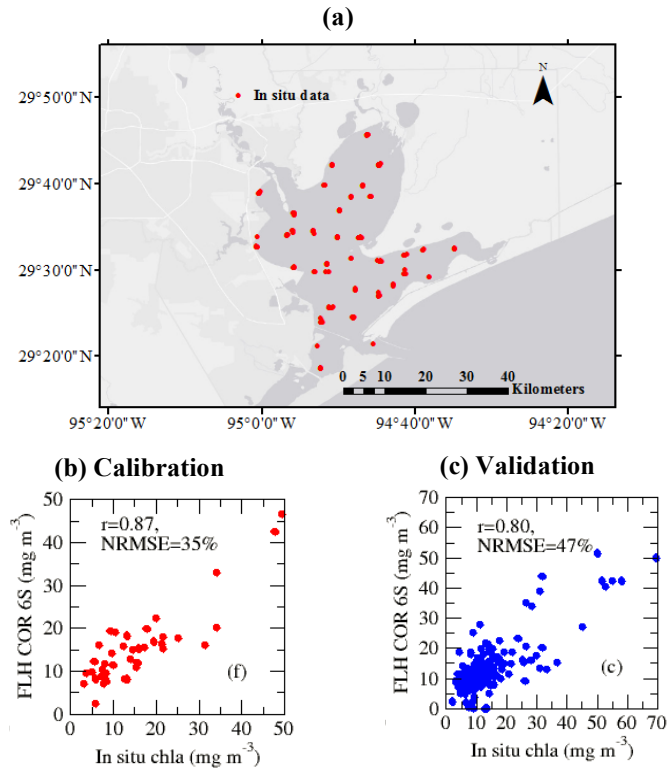


**Figure 3-1.** MERIS data calibrated and validated against in-situ data. (a) The locations of chla sampling sites; (b) chla calibration results; (c) chla validation results. FLH is Fluorescence Line Height;  $r$  is coefficients of correlation; NRMSE is Normalized Root-Mean Square Error. Reprinted from (Zhang *et al.* 2016).

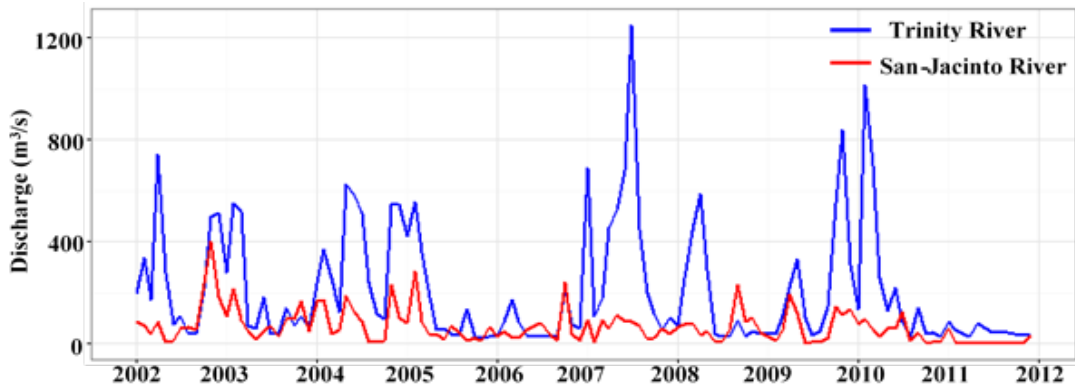


**Figure 3-2.** Monthly discharge from the Trinity River and the San Jacinto River.

Hourly water temperature data is acquired from Texas Water Development Board (TWDB). Because there is no significant difference among water temperature values over different locations (Appendix A), the data collected at Boli monitoring station (29.34° N, 94.78° W) are chosen to represent the water temperature in the bay. For data continuity, missing observation data is filled using water temperature from other stations such as Midg (29.51° N, 94.88° W) and Trin (29.66° N, 94.75° W).

Hourly air temperature data are also downloaded from NOAA (Station# WBAN 12923, GALVESTON SCHOLLS FIELD TX US). The hourly data are then averaged to monthly for deriving the relationship between air temperature and water temperature, such that water temperature (which is difficult to predict) can be inferred from air temperature through seasonal forecasts.

The MEI is used to represent the intensity of an ENSO event in this thesis. As one of the most comprehensive indexes for monitoring ENSO, MEI combines multiple meteorological and oceanographic components, including sea-level pressure, surface



wind, sea surface temperature, air temperature, and total cloudiness fraction of the sky (NOAA, <https://www.esrl.noaa.gov/psd/enso/mei/>).

## 3.2 Methods

### 3.2.1 Segments division

In this study, it is assumed that inland-adjacent segments (northern segments) of Galveston Bay are more affected by river discharge than the southern parts. To better represent the influence of freshwater inflow, the research area is divided into five sub regions based on chl<sub>a</sub> spatial distributions and hydrodynamic conditions over Galveston Bay, as simulated by the Environmental Fluid Dynamics Code (EFDC) during the period of January 1<sup>st</sup>, 2005 to December 31<sup>th</sup>, 2006 (Shen *et al.* 2016). The simulation results from EFDC demonstrate the flow direction in the bay, which is from the Trinity River and the San Jacinto River to the Houston Ship Channel. These sub-regions are Trinity Bay, San Jacinto Bay, East Bay, Lower Bay, and West Bay (Figure 3-3). This study explores the key factors driving chl<sub>a</sub> and constructs a prediction model using these factors in each of the five segments.

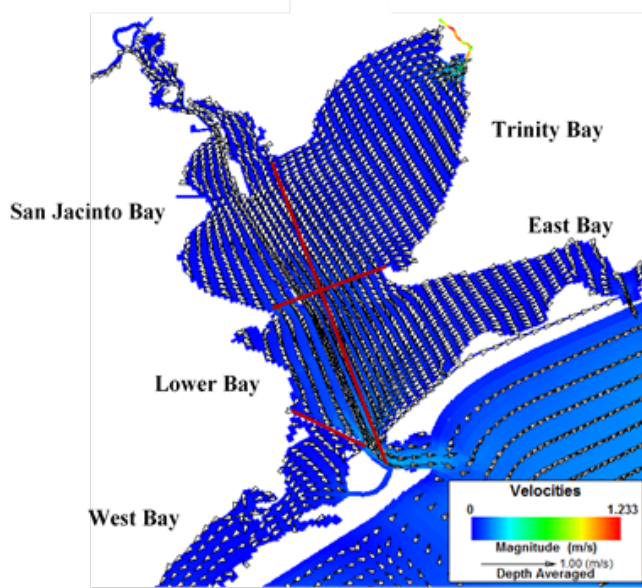


**Figure 3-3.** The segments are divided based on hydrodynamic simulation results from the Environmental Fluid Dynamics Code (EFDC) (white arrows represent the flow direction and color means magnitude of flow velocities).

### 3.2.2 Chla spatiotemporal analysis

In this part, chla data from May 21<sup>th</sup>, 2002 to December 31<sup>th</sup>, 2011 are analyzed to identify the spatial/temporal distributions of the chla concentrations in Galveston Bay. The inter-annual and monthly distribution patterns of chla are examined. Annual and monthly time series of chla in all of these segments are compared as well.

For better understanding the chla spatial-temporal variations, monthly and annual Standard Deviation (SD) patterns will be calculated after equation (3-1).

$$SD = \sqrt{(x - \bar{x})^2 / N} \quad (3-1)$$

Where  $x$  is the monthly or annual chla value in each grid;  $\bar{x}$  is the monthly or annual mean value;  $N$  is the number of months or years. Furthermore, time series analysis is conducted for each segment.

### 3.2.3 Chla driving factors analysis

In this section, correlation and linear regression analyses are applied to identify the key environmental factors driving chla variations in different seasons over different segments.

In this study, seasonal groups are divided up based on the correlation performance between discharge and chla. The result shows that four seasonal groups perform the best among the different division methods: (1) JFM – January, February and March; (2) AMJ – April, May and June; (3) JAS – July, August and September; (4) OND – October, November and December. For all four seasonal groups, chla anomalies, freshwater inflow anomalies, and water temperature anomalies are calculated by subtracting their monthly climatological values. The correlation coefficients are then compared and ranked for each season such that the most influential factors can be identified.

The relative importance of multiple variables is evaluated by conducting a relative weight analysis (Johnson 2000). By using a variable transformation approach, a new set of predictors that are orthogonal to one another is created to eliminate the effects of multicollinearity among variables. Then the criterion of these new orthogonal predictors can be established and the resulting standardized regression coefficients can be calculated. Last,

these standardized regression weights are transformed back to the metric of the original predictors (see Figure 3-4 and equation (3-2)) (Tonidandel and LeBreton 2011). In this study, relative weight analysis is done based on hier.part package in R (Grömping 2006).

$$\varepsilon_i = \beta_1^2 \lambda_{i1}^2 + \beta_2^2 \lambda_{i2}^2 + \beta_3^2 \lambda_{i3}^2 \quad (3-2)$$

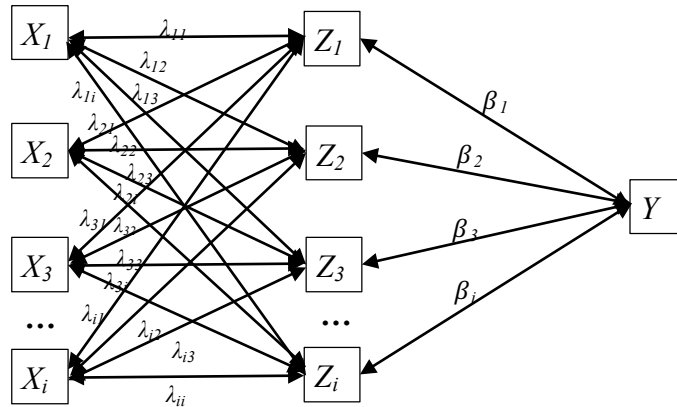


**Figure 3-4.** Calculation of relative weights for a regression model with three predictors. Modified from (Johnson 2000).

Where  $X_i$  are the  $i^{th}$  original predictor;  $Z_i$  are new orthogonal predictors;  $\beta_i$  is the  $i^{th}$  set of standardized regression coefficients;  $\lambda_{ik}$  is obtained by regressing  $X_i$  on the set of  $Z_{Xk}$ ;  $\varepsilon_i$  is relative weight after summing squared standardized regression coefficients  $\beta_k^2$  and  $\lambda_{ik}^2$ .

### 3.2.4 Constructing a chla prediction model

By establishing and validating the quantitative relationships between the chla concentrations and key environmental drivers, future chla concentrations can be simulated

using the predictions of these environmental variables. The prediction model is further validated against observations, making it practical for provide effective scientific supports for future decision making for coastal protection. Also, all methods developed in this study are transferrable, which could be applied in other coastal regions.

Monthly chla concentrations can be treated as the sum of two terms: monthly climatology and monthly anomaly. It is assumed that the chla anomalies are affected by inflow anomaly, water temperature anomaly, and MEI. Monthly freshwater inflow and water temperature anomalies can be calculated by subtracting their monthly averages and used to derive the prediction equations of chla anomaly. Therefore, chla concentration can be estimated using the following equations.

$$C_{chla} = C_{clim} + C_{anom} \quad (3-3)$$

$$C_{anom} = f_1 (Q_{anom}, T_{wanom}, MEI) \quad (3-4)$$

$$T_{water} = f_2 (T_{air}) \quad (3-5)$$

Where  $C_{chla}$  is the chla concentration;  $C_{clim}$  is the climatological average value of chla,  $C_{anom}$  is the chla anomaly;  $Q_{anom}$  is the river discharge anomaly;  $T_{wanom}$  is the water temperature anomaly; MEI is the Multiple ENSO Index value from NOAA; and  $T_{water}$  and  $T_{air}$  are the water temperature and air temperature, respectively.

A multiple variable regression analysis is used to develop the prediction model. In addition to the traditional multiple regression analysis, stepwise regression of backward elimination is used to reduce the influence of collinearity among environmental factors (Derksen and Keselman 1992).

The datasets are divided into two parts: the first seven years of data (from January 2002 to December 2008) are used for training while the last three years of data (from January 2009 to December 2011) are used for testing.

## 4. RESULTS

### 4.1 Spatial and Temporal Variability of Chla

#### 4.1.1 Spatial distribution of chla

According to the historical remotely sensed data from MERIS (2002 – 2011), the annual and monthly chla spatial distributions share some common features (Figure 4-1(a) & 4-2(a)). In general, high chla concentration levels are usually found near the shoreline, which may be caused by several factors, such as large biomass accumulations, reflections from the land and the imperfect chla-deriving model without considering the shallow bottom reflection (Barnes *et al.* 1995; Dzwonkowski *et al.* 2005) or imperfect atmospheric corrections. Yet in the center part of the bay, the chla is relatively low, especially around where the Houston Ship Channel (HSC) is located. The HSC is about three times deeper than the other parts of the bay (Figure 2-1). In this region, algae growth is limited because the water column is well-mixed, resulting in a low nutrient concentration (as compared to the other, shallower parts). Additionally, the chla concentrations at the mouths of the Trinity River and San Jacinto River are generally lower than that in the other parts of the bay, which may be because the environment is not optimal for algae growth, mainly due to the water disturbance from freshwater inflows (which leads to a high turbidity and a small amount of light penetration). This is especially true for the Trinity River, whose large inflow increasingly stimulates circulation and the transport of nutrients further into the bay – which restrains the algae growth, and reduces the accumulation of plankton

biomass around the river outlet. In contrast, for the areas in Trinity and San Jacinto Bays which are between river outlets and the HSC, higher chla concentrations are usually found due to lower water velocity, lower salinity content, more nutrient accumulation, and higher light penetration levels as compared to the outlet and the parts near HSC.

The chla concentrations in the northern segments (14.64 µg/L averagely in Trinity Bay and 15.44 µg/L in San Jacinto Bay) are higher than that of the southern parts (13.49 µg/L in East Bay, 13.15 µg/L in Lower Bay and 11.75 µg/L in West Bay). This suggests that areas adjacent to the Gulf of Mexico are less affected by river inflows (Figure 4-3). San Jacinto Bay – which is adjacent to Houston area – usually has higher chla concentrations than other four segments. It is perhaps because this region receives more wastewater directly with higher nutrients concentrations than Trinity Bay did (Armstrong *et al.* 1993). The lowest chla is observed in West Bay, both annually and monthly. This is mainly caused by the narrow shape around that area, where freshwater exchange is limited and relatively high salinity concentration is maintained (23 ppm on average, which is higher than the salinity in northern parts with around 10 ppm).



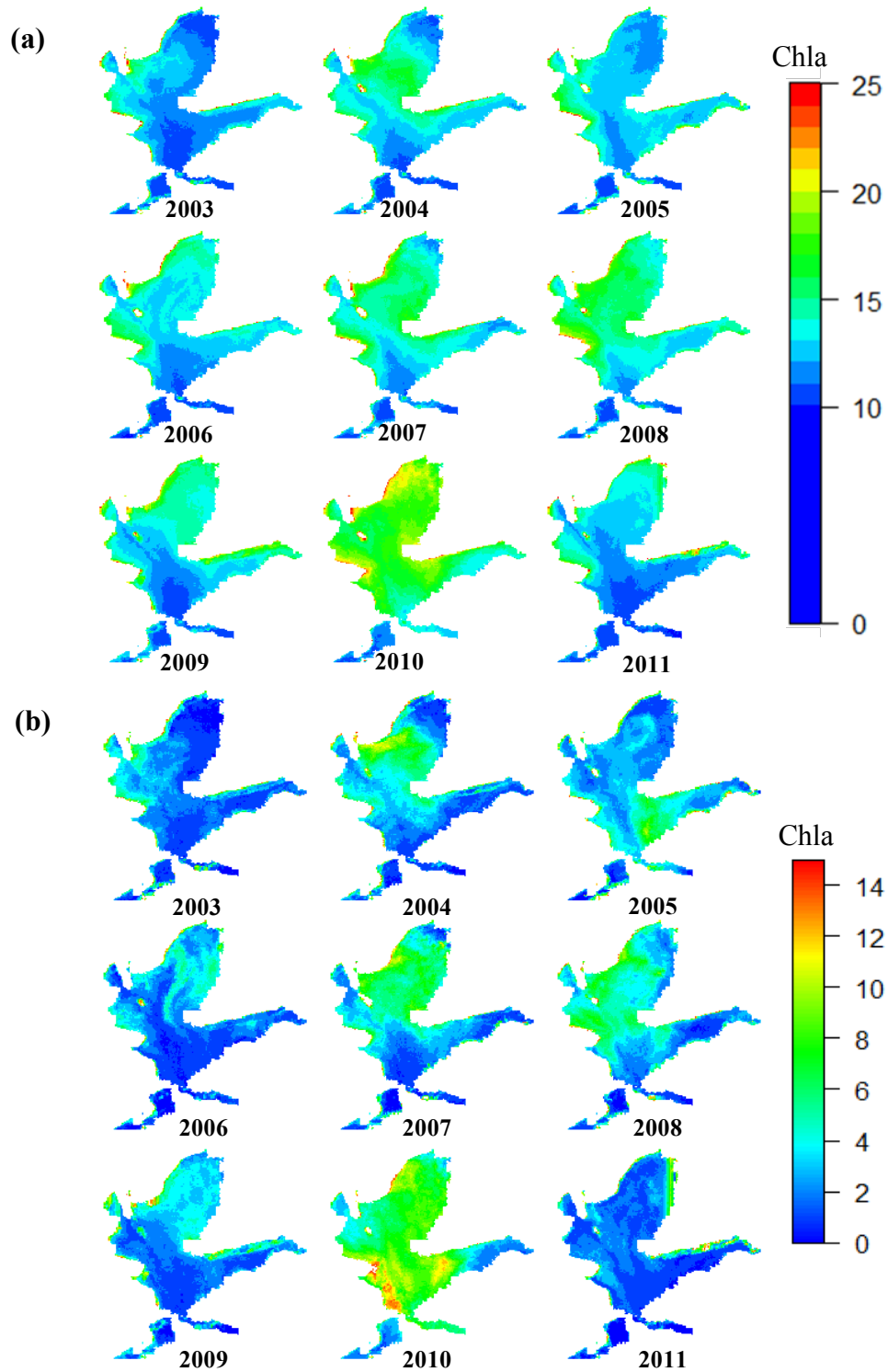


**Figure 4-1.** Annual chl a spatial distributions. (a) Mean chl a concentrations by year; (b) Standard deviation of chl a concentrations by year. Units:  $\mu\text{g/L}$  (2002 is excluded because of data limitation).

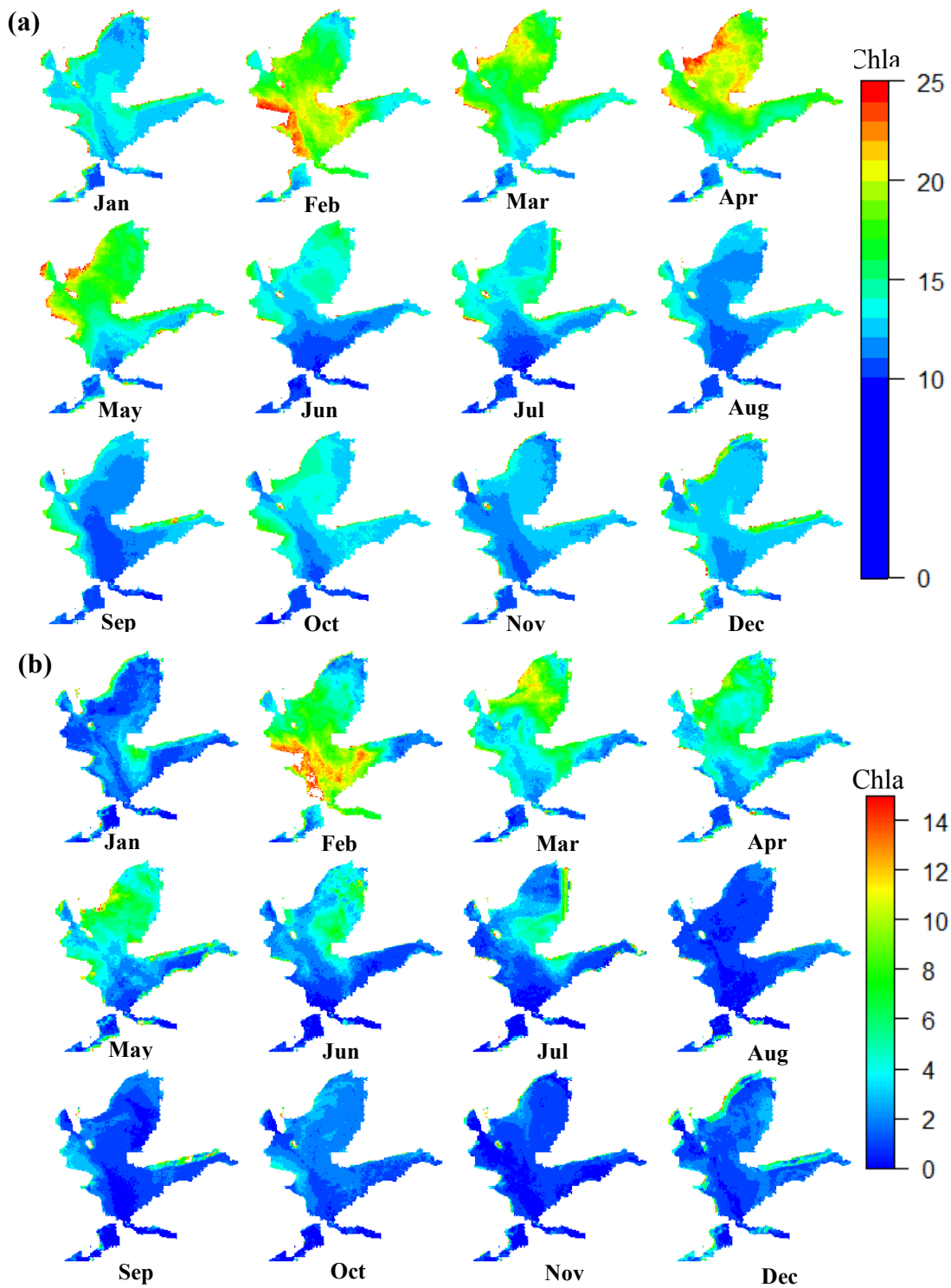


**Figure 4-2.** Monthly chl a spatial distributions. (a) Mean chl a concentrations by month; (b) Standard deviation of chl a concentrations by month. Unit:  $\mu\text{g/L}$

#### 4.1.2 Inter-annual variability of chla

Temporal variations of chla are key for exploring the impacts of environmental factors on plankton biomass. Annual mean chla patterns are shown in Figure 4-1 & Figure 4-3(a). The result suggests a strong inter-annual variability of chla in Galveston Bay. In general, the chla concentration tends to increase for all five segments during the study period (except for 2009 and 2011). Overall, the highest chla concentration appears in 2010 (a wet year), then followed by a sharp decrease in 2011 (a drought year).

The inter-annual chla variability is further analyzed and quantified through time series analysis (Figure 4-3(a)). Comparing San Jacinto Bay with Trinity Bay, it is obvious that the average of annual mean chla in San Jacinto Bay is consistently higher than Trinity Bay (except in 2009 and 2010), with the range from 13.67  $\mu\text{g/L}$  in 2009 to 16.60  $\mu\text{g/L}$  in 2010. For Trinity Bay, it ranges from 12.03  $\mu\text{g/L}$  in 2003 to 18.17  $\mu\text{g/L}$  in 2010. The largest difference between those two segments occurs in 2005 when chla in San Jacinto Bay is about 2.50  $\mu\text{g/L}$  higher than that in Trinity Bay. East Bay, adjacent to Trinity Bay, has relatively high chla (from 11.79  $\mu\text{g/L}$  in 2011 to 16.02  $\mu\text{g/L}$  in 2010) as compared to Lower Bay, which is next to San Jacinto Bay. However, there is no major difference between East Bay and Lower Bay. Consistent with the spatial patterns shown in Figure 4-1, West Bay has low and steady chla concentrations (range from 11.01  $\mu\text{g/L}$  in 2011 to 11.93  $\mu\text{g/L}$  in 2009) during the entire periods, largely attributed to the effects of seawater flushing.

#### 4.1.3 Monthly variability of chla

Similar to the results from inter-annual variability, Figure 4-2 and Figure 4-3(c) show the distribution patterns of monthly climatology. Both the distribution patterns and the time series of chla reveal clear seasonal variation patterns. Chla concentration observably fluctuates with the highest values occurring from February to May. For most of the time during the year, the high values tend to cluster around the northern segments (except for February when the largest chla concentration occurs in the center of the bay) (Figure 4-2(a)). Higher monthly mean chla concentrations are also accompanied by higher seasonal standard deviations (Figure 4-2(b)). For instance, the chla concentrations in February are relatively high values across the whole bay and the standard deviations of chla in February are also found to be the highest among all of the months. In addition, from August to the following January, the spatial distribution of chla is more homogeneous as compared to the other months (especially from February to May).

Among the different segments, San Jacinto Bay usually has higher chla concentrations the year round, following by Trinity Bay, East Bay, Lower Bay, and West Bay. This phenomenon is similar with the inter-annual variation situation (Figure 4-1(b) and 3(b)). In April, chla concentration reaches its annual maximum value in both Trinity Bay (19.82  $\mu\text{g/L}$ ) and San Jacinto Bay (19.26  $\mu\text{g/L}$ ). However, in other segments, the highest values occur in February (18.07  $\mu\text{g/L}$  in East Bay, 19.57  $\mu\text{g/L}$  in Lower Bay and 13.92  $\mu\text{g/L}$  in West Bay). This spatial pattern indicates that algal blooming season lasts two month longer in the northern segments than the southern segments. The seasonal

variability also demonstrates that the spring algal blooming in Galveston Bay occurs from February to April. Afterwards, the chl<sub>a</sub> concentrations begin to decrease until the end of the year. Many factors may contribute to this phenomenon. For example, relatively higher temperature and more solar radiation in this subtropical region may shift the algal blooming season to an earlier date (beginning in February); freshwater inflow may bring more nutrients, stimulating the continuous growth of chl<sub>a</sub> in northern area of the bay after the spring blooming. When the dissolved oxygen in the spring is consumed by biomass accumulation or reduced from the rising water temperature, further algal growth will be limited and a decline of chl<sub>a</sub> concentrations usually start from May.

According to the above analysis, the chl<sub>a</sub> spatial and temporal variations are affected by multiple environmental factors, such as freshwater inflow, nutrients input, temperature, topography condition, and algal growth cycling, etc. Each of those factors has interactions with any of others. The combined effects from those factors make it difficult to identify the key drivers of chl<sub>a</sub> spatial and temporal variability. To provide a practical approach for predicting chl<sub>a</sub> in supporting ecological management practice in Galveston Bay, further analysis is needed to quantify the correlations and interactions between chl<sub>a</sub> and its environmental driving factors.

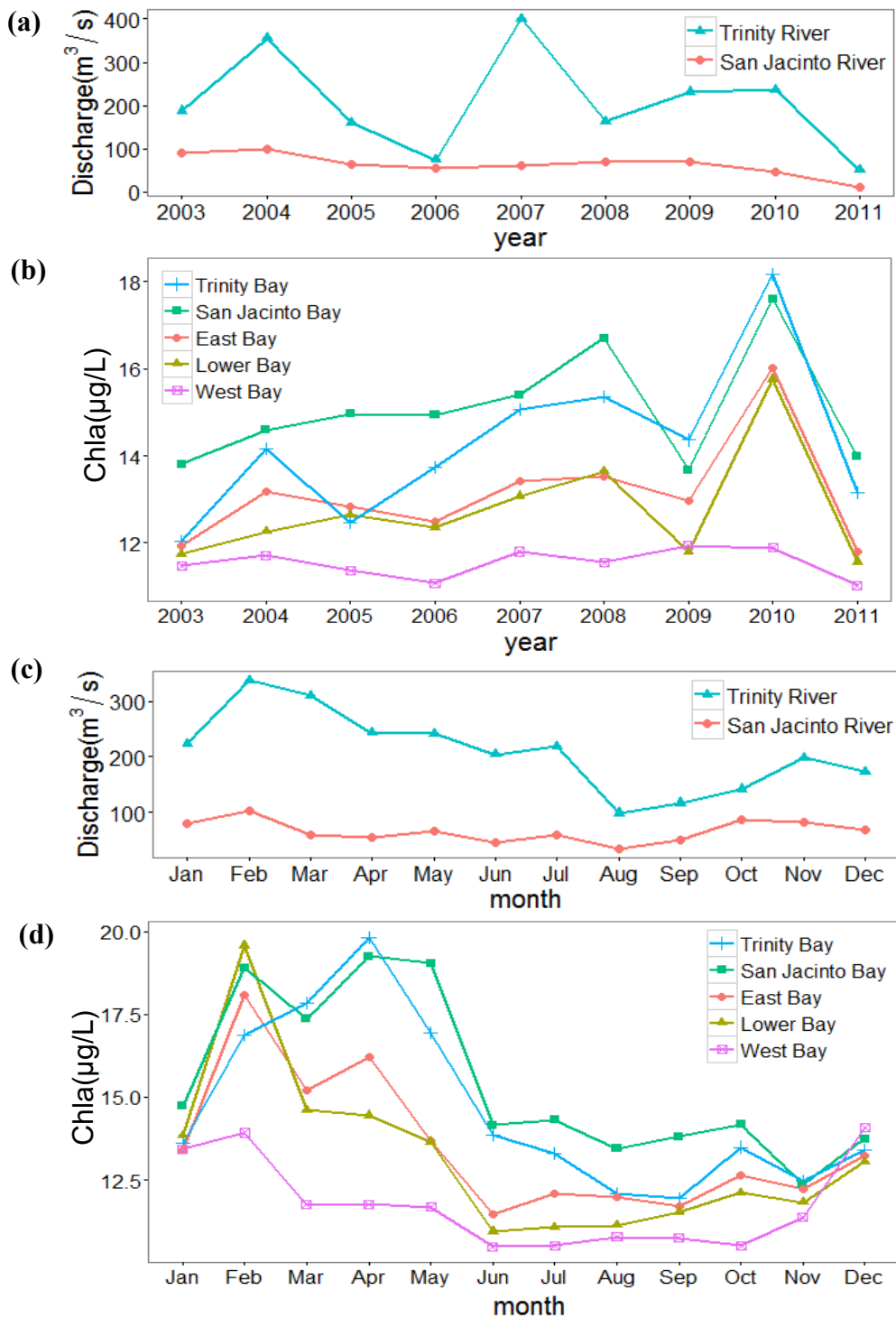
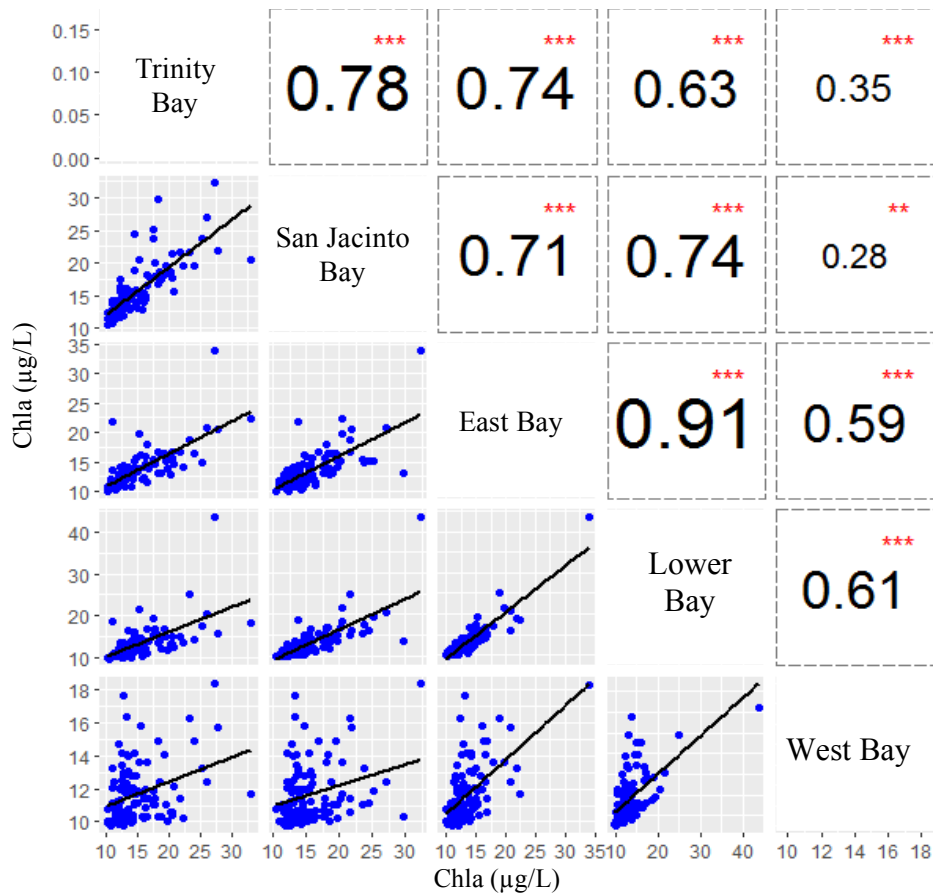


**Figure 4-3.** Time series of chl a and discharge over May 2002 to December 2011. (a) Annual mean discharge; (b) Annual mean chl a; (c) Monthly climatology of discharge; (d) Monthly climatology of chl a.

## 4.2 Chla Driving Factors: Freshwater Inflow and Climate Conditions

Figure 4-4 shows that chla in all five segments are correlated with each other. In addition, the highest correlation is found between East Bay and Lower Bay, followed by that between Trinity Bay and San Jacinto Bay. Considering the northern segments are more affected by freshwater compared with the southern parts, Trinity Bay and San Jacinto Bay are chosen as the focused area in this thesis.



Significant codes:  $p < 0.001$  \*\*\*;  $0.001 < p < 0.01$  \*\*,  $0.01 < p < 0.05$  \*,  $0.05 < p < 0.1$  .

**Figure 4-4.** The chla correlations among segments.

#### 4.2.1 Freshwater inflow

Roelke *et al.* (2013) suggested that upstream inflows (e.g., magnitude, timing and frequency) might have a profound influence on biomass accumulation in Galveston Bay. To further quantify the relationship, correlation analysis is conducted between the remotely sensed chl<sub>a</sub> and the observed freshwater inflow in Trinity and San Jacinto segments.

Over both Trinity Bay and San Jacinto Bay, the chl<sub>a</sub> concentrations show positive correlations with the inflow from the Trinity River. Specifically, as shown in Figure 4-3, the correlation coefficient (R) between the monthly chl<sub>a</sub> climatology in Trinity Bay and the inflow from the Trinity River is 0.75 ( $p < 0.01$ ), and the R between the monthly chl<sub>a</sub> climatology in San Jacinto Bay and the Trinity River discharge is 0.73 ( $p < 0.01$ ). This positive correlation indicates that chl<sub>a</sub> concentration is relatively high during the wet season (from February to May) and relative low during the period when the region is dry (from August to December).

From the time series over these two segments (Figure 4-5), the annual cycles of both chl<sub>a</sub> and discharge can be observed. The highest chl<sub>a</sub> concentrations for these two segments both occur around March in 2010. While a strong positive correlation is found between the freshwater inflow from the Trinity River and the monthly chl<sub>a</sub> in Trinity Bay ( $R = 0.57, p < 0.01$ ), the discharge from the San Jacinto River has little impacts on chl<sub>a</sub> concentration in San Jacinto Bay ( $R < 0.1$ ). When the San Jacinto River discharge rate is less than 100 m<sup>3</sup>/s, the chl<sub>a</sub> concentrations over San Jacinto Bay increase slightly as the



discharge increases. However, when freshwater inflow exceeds 100 m<sup>3</sup>/s, chla concentrations are barely affected by the discharge. These results suggest that the correlation between freshwater inflow and chla varies significantly by locations. In addition to the discharge volume received by the bay segment, the light levels, water stability, turbidity, and nutrient input are all affected by flushing.

The above analysis suggests that the discharge from the Trinity River affects both Trinity Bay and San Jacinto Bay. The discharge from the Trinity River is about three times larger, on average, than that from the San Jacinto River (Figure 4-5). Given the circulations in the bay, the Trinity River can significantly influence the chla dynamics across the entire bay. In addition to the volume of discharge, other factors may also play important roles in driving chla concentration variabilities, such as location, topographic condition, flow circulation, and tidal action.

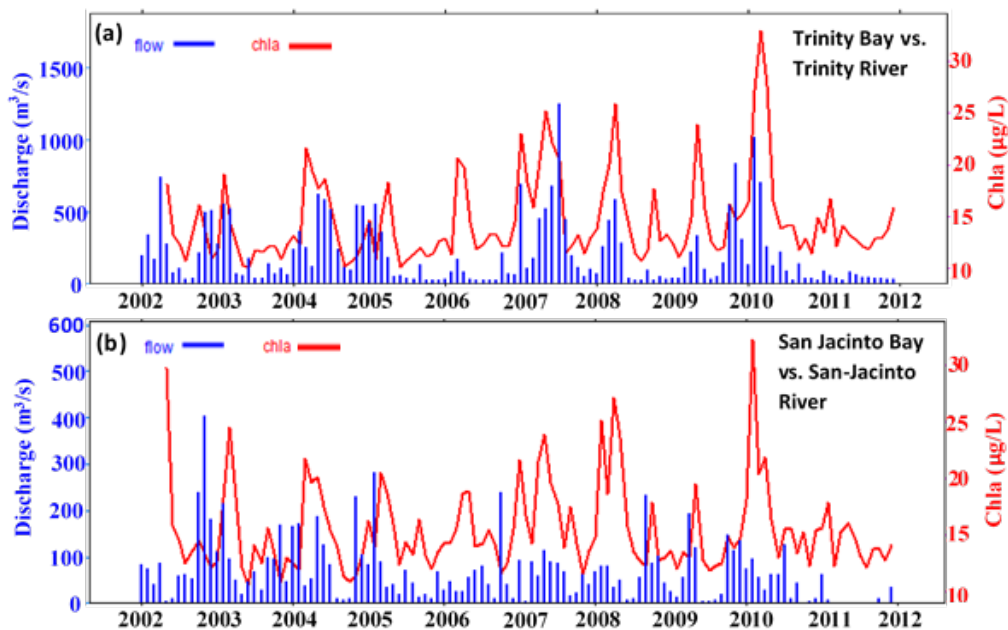


**Figure 4-5.** Time series of monthly discharge and chla concentration in (a) Trinity Bay and (b) San Jacinto Bay.

#### 4.2.2 Climate conditions

As mentioned in Section 1.1, climate conditions can significantly influence the chl<sub>a</sub> variability by driving other parameters, such as water temperature and river discharge. Here we focus on examining the impacts associated with water temperature and MEI – an index for diagnosing ENSO – on chl<sub>a</sub> in Galveston Bay. Figure 4-6 shows the time series of monthly MEI, water temperature anomalies, and chl<sub>a</sub> concentration anomalies. The result shows that there is no significant correlation between MEI and chl<sub>a</sub> anomaly ( $R < 0.1$  for both segments). However, as an important indicator of climatic variability, the water temperature anomaly shows the significant negative impact on chl<sub>a</sub> concentration anomaly in Trinity Bay ( $R = -0.35$ ) and San Jacinto Bay ( $R = -0.33$ ). This is in contrast to research results which show positive impacts from water temperature on chl<sub>a</sub> in other bay areas (Rheuban *et al.* 2016; Korosov *et al.* 2015).

The correlations in both locations are significant (with  $p < 0.001$ ), indicating the overall negative influence of water temperature on algal growth. Usually the highest temperature within one year in Galveston Bay occurs in August (~31 °C), when the chl<sub>a</sub> concentrations are typically low. The chl<sub>a</sub> concentrations usually peak around 22°C (in April), which corresponds to the optimum growth temperature range of most algae species. Then chl<sub>a</sub> tends to decrease when the water temperature is above 25 °C after May (the Optimum growth temperature of Cyanobacteria). This phenomenon agrees with the temporal chl<sub>a</sub> variabilities observed from Figure 4-6. It is also similar with findings from other studies carried out in Galveston Bay (Örnólfsson *et al.* 2004).

In summary, chl<sub>a</sub> variabilities are mainly driven by discharge anomalies of the Trinity River and water temperature anomalies, while MEI does not have noticeable impact on the chl<sub>a</sub>.

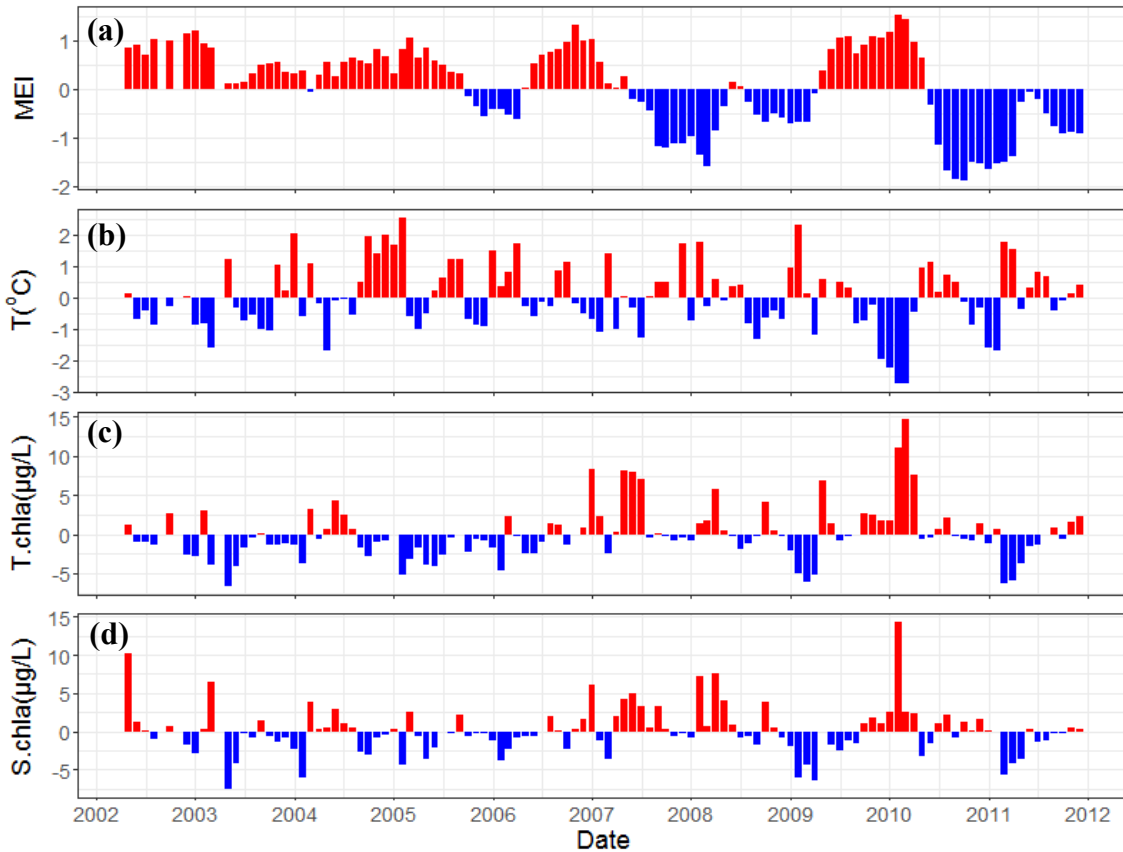


**Figure 4-6.** Time series of (a) MEI (blue represents La Niña and red is for El Niño); (b) water temperature anomalies; (c) chl<sub>a</sub> anomalies from Trinity Bay; (d) chl<sub>a</sub> anomalies from San Jacinto Bay.

#### 4.2.3 Seasonal correlation between chl<sub>a</sub> and environmental factors

As explained in Chapter 3.2.3, four seasonal groups (JFM, AMJ, JAS and OND) are chosen to further develop multiple correlation and regression analysis. The correlation

coefficients between the Chlorophyll-a anomalies and the anomalies of the aforementioned environmental factors were then compared and ranked for each season, such that the most influential factors for each segment could be identified. The results for different seasonal groups are shown in Figure 4-7 (Trinity Bay and San Jacinto Bay), Figure 4-9 (East Bay and Lower Bay), and Figure 4-10 (West Bay).

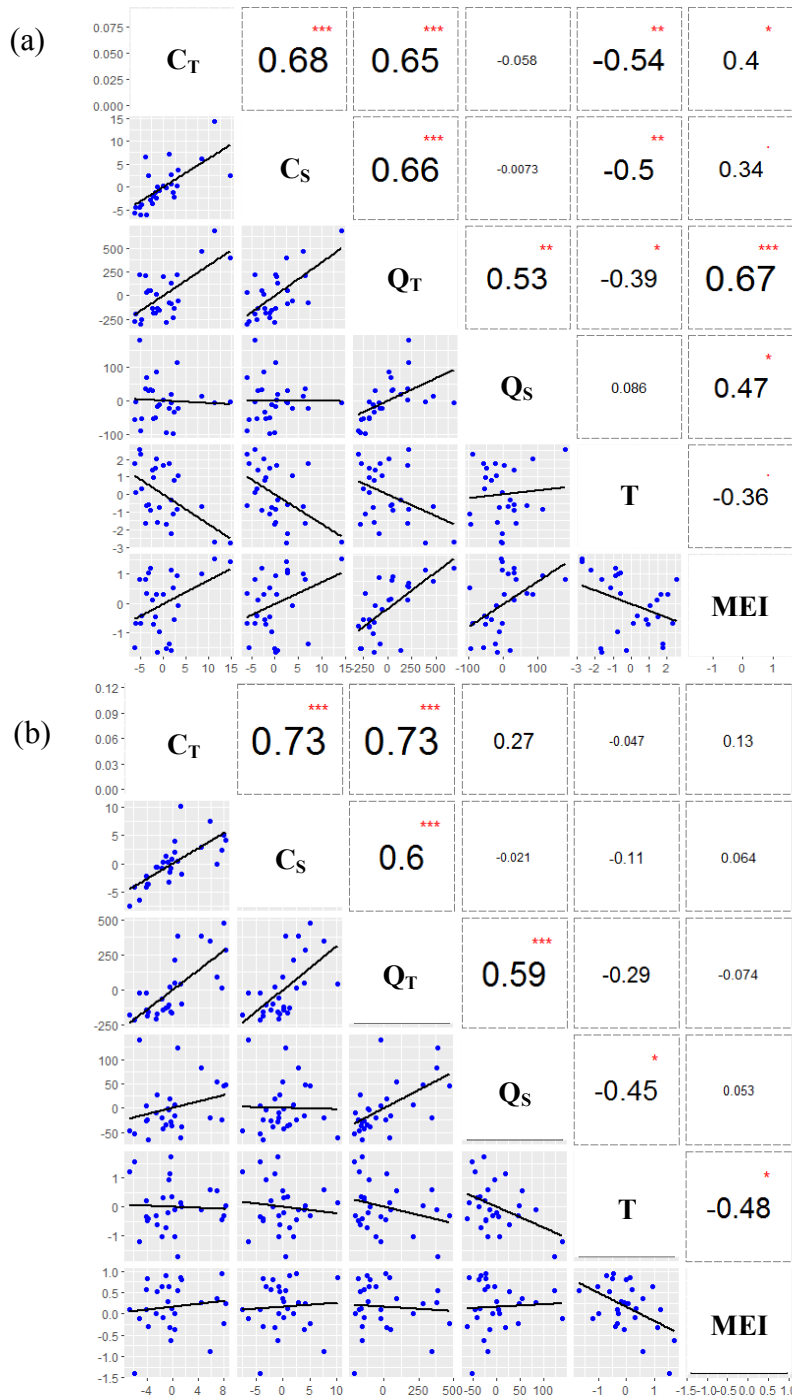
(1) Trinity Bay and San Jacinto Bay

Compared with the discharge from the San Jacinto River, the discharge from the Trinity River has the larger impact on the chl<sub>a</sub> concentrations in both segments in most seasons (except for OND). This result confirms the dominant role of discharge from the Trinity River on chl<sub>a</sub> across the bay, even though San Jacinto Bay receives discharge from the San Jacinto River directly. This may be attributed to the large freshwater inflow amount from the Trinity River and the mixing of the Trinity inflow in the whole bay – not just around the adjacent area. Thus, for establishing the predication model, discharge from the Trinity River will be used as the main freshwater driver in both two northern segments.

In addition, significant negative correlations are shown between water temperature and chl<sub>a</sub> both in Trinity Bay and San Jacinto Bay, especially in JFM and OND ( $p < 0.01$ ). However, for AMJ and JAS, chl<sub>a</sub> variability is less affected by water temperature (Figure 4-7(b) & (c)). Thus, for different seasonal groups, the main driving factors are different. In JFM, both discharge and water temperature have significant influence on chl<sub>a</sub> concentrations. In AMJ and JAS, chl<sub>a</sub> is most affected by discharge from the Trinity River. In OND, the volume of discharge is low in general. Water temperature may act as the limiting factor for algal growth, and the primary driver for chl<sub>a</sub> concentration. Thus, water

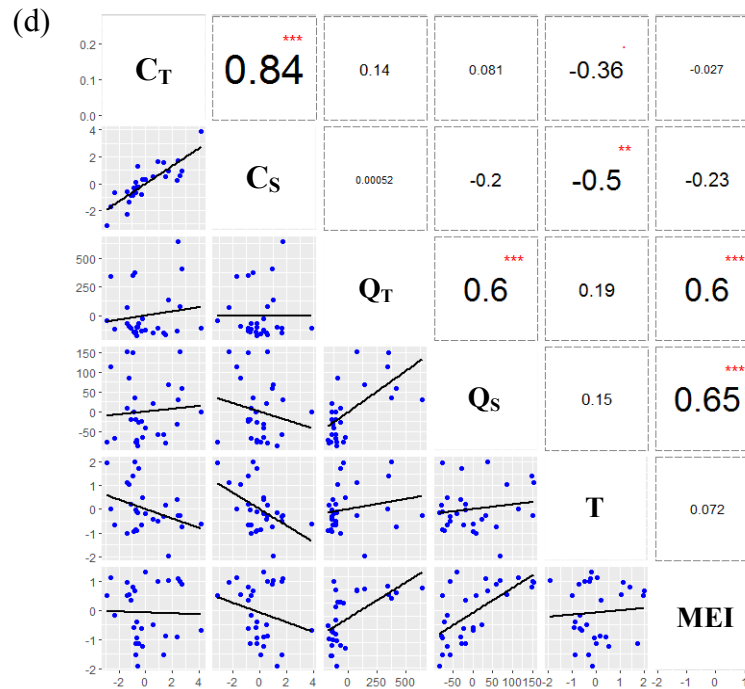
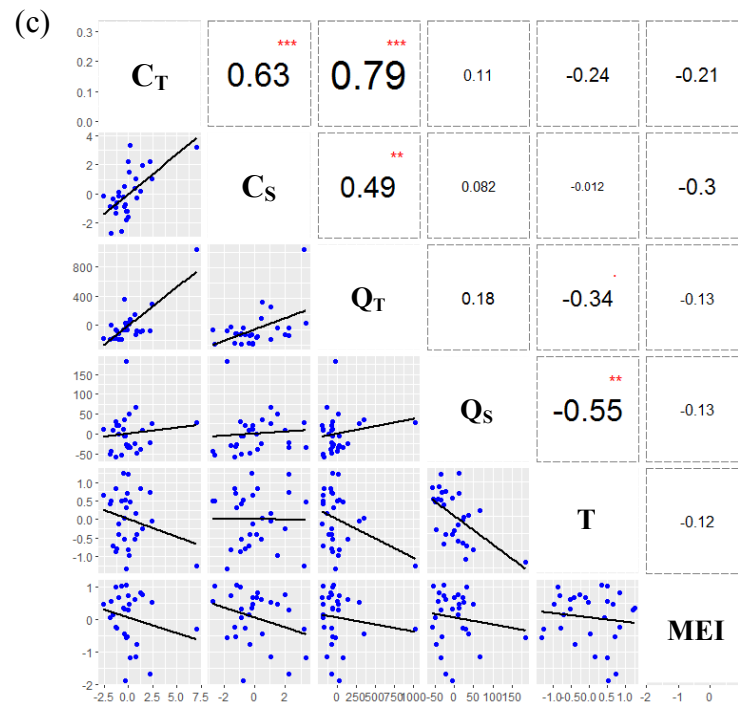
temperature would be more significant than discharge to drive chla concentration. The high positive water temperature anomaly during a dry year (with less discharge) is associated with less dissolved CO<sub>2</sub> and O<sub>2</sub> in the waterbody, which might lead to a decrease in the chla concentration (Chavez *et al.* 1999). Therefore, it is necessary to develop the prediction equations of chla concentrations using different factors based on different seasonal groups.

In addition, the multiple correlation analysis (Figure 4-7) shows that the correlations also exist among the selected environmental factors. For instance, positive correlations are found between MEI and river discharge anomaly in JFM and OND ( $p < 0.05$ ). Similar phenomenon is also observed between water temperature and MEI, and between the inflows from the two rivers.



Significant codes:  $p < 0.001$  \*\*\*;  $0.001 < p < 0.01$  \*\*;  $0.01 < p < 0.05$  \*;  $0.01 < p < 0.1$

**Figure 4-7.** The monthly average correlation among  $C_T$  (chl<sub>a</sub> anomaly in Trinity Bay,  $\mu\text{g/L}$ ),  $C_S$  (chl<sub>a</sub> anomaly in San Jacinto Bay,  $\mu\text{g/L}$ ),  $T$  (water temperature anomaly,  $^{\circ}\text{C}$ ),  $MEI$  (Multiple ENSO Index from NOAA),  $Q_T$  (discharge anomaly from the Trinity River,  $\text{m}^3/\text{s}$ ) and  $Q_S$  (discharge anomaly from the San Jacinto River,  $\text{m}^3/\text{s}$ ) in (a) JFM; (b) AMJ; (c) JAS and (d) OND.



Significant codes:  $p < 0.001$  \*\*\*;  $0.001 < p < 0.01$  \*\*;  $0.01 < p < 0.05$  \*;  $0.01 < p < 0.1$  .  
 Figure 4-7. Continued.

The relative importance of discharge from the Trinity River, water temperature and MEI on chla anomalies in the four seasonal groups are shown in Figure 4-8. In AMJ and JAS, discharge acts as the dominant factor in determining the chla concentration. In OND, chla is mainly determined by water temperature in both Trinity Bay and San Jacinto Bay. In JFM, chla concentrations are affected by the combining effects of all factors, especially from discharge and water temperature. This analysis about the relative importance of predictor variables can help improve the understanding of the chla variability and explore its causes. This is an important step towards developing the chla prediction model.

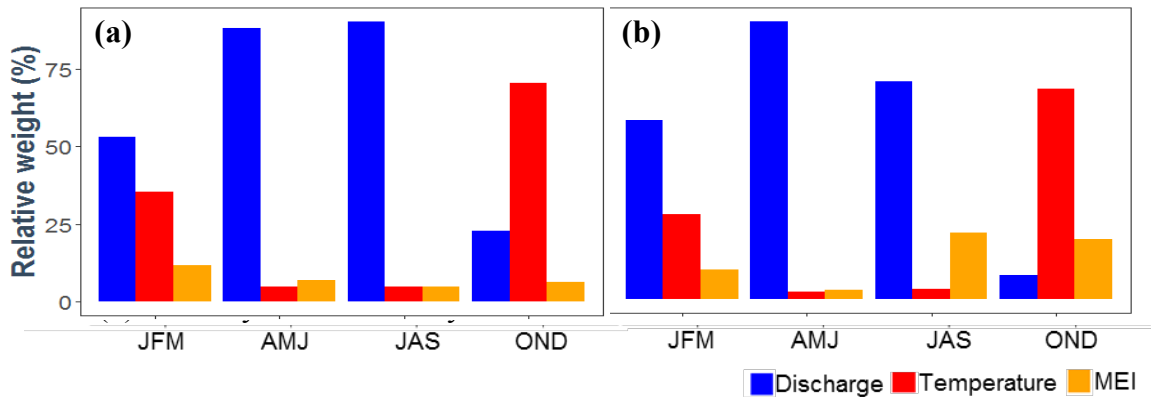


**Figure 4-8.** Relative Importance of Predictor Variables (discharge from the Trinity River, water temperature and MEI) in (a) Trinity Bay; (b) San Jacinto Bay.

## (2) East Bay and Lower Bay

In both East Bay and Lower Bay, chla is mainly correlated with the discharge from the Trinity River ( $0.5 \leq R \leq 0.8$ ), with the exception in OND in Lower Bay. In addition, significant negative correlations are found between water temperature and chla, especially in JFM ( $R = -0.47$  in both segments,  $p < 0.01$ ). In JFM, positive correlation can be



observed between MEI and chl<sub>a</sub> (with  $R = 0.64$ ) in the Bay and ( $R = 0.49$ ) in Lower Bay. However, for AMJ and JAS, chl<sub>a</sub> is mainly determined by discharge from the Trinity River (Figure 4-11(b) & (c)).

Similar to the two northern segments, correlations are also found among the environmental factors. For instance, positive correlations are found between MEI and river discharge anomaly in JFM and OND ( $0.47 \leq R \leq 0.67$ ,  $p < 0.01$ ).

The relative importance analysis in Figure 4-11 shows that discharge from Trinity Bay is the primarily dominant factor in driving chl<sub>a</sub> concentration in East Bay. Its relative weight are above 50% in all of four seasonal groups (from 51.21% in JFM to 86.74% in JAS). However, for Lower Bay, discharge is the main driver in all seasons except for OND. In OND, temperature is the key dominant impacting factor of chl<sub>a</sub>.

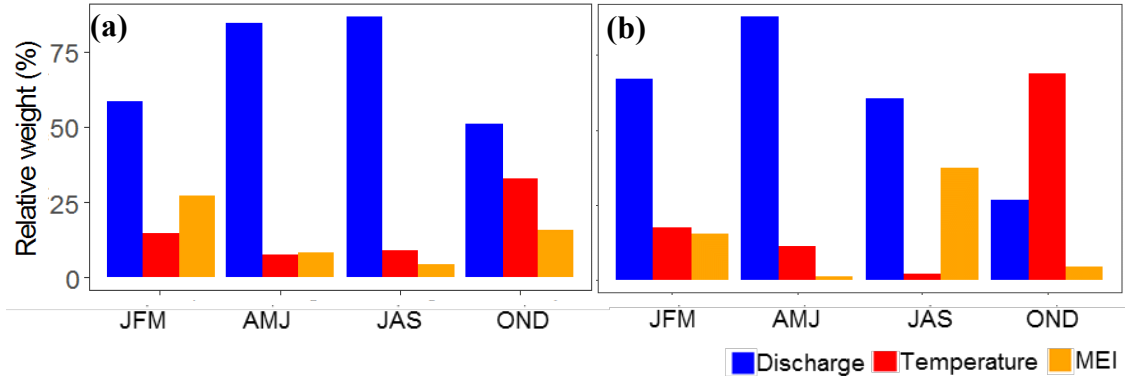


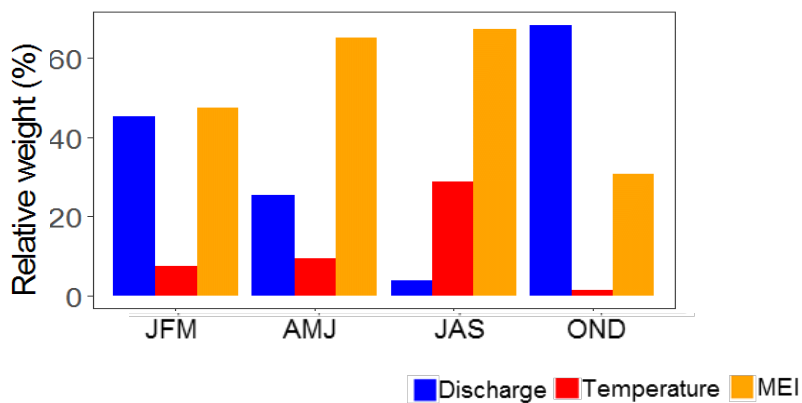
**Figure 4-9.** Relative Importance of Predictor Variables (discharge from the Trinity River, water temperature and MEI) in (a) East Bay and (b) Lower Bay.

### (3) West Bay

Figure 4-12 shows the results for West Bay. In JFM, both discharge of the Trinity River and MEI show the significant correlation with chl<sub>a</sub> ( $R = 0.62$  for discharge and  $0.63$  for MEI,  $p < 0.001$ ). In addition, these two factors are well correlated ( $R = 0.67$ ,  $p < 0.001$ ).

In AMJ, only MEI has some small effect on chla. In OND, the discharge from the Trinity River influences chla positively ( $R = 0.39, p < 0.05$ ). However, in JAS, no obvious correlation is found between any of the factors and chla.

Figure 4-10 shows the similar result that MEI has the impact on chla in JFM and AMJ (47.51% and 65.39%, respectively). Even though there is no clear correlation between any of the factors with chla in JAS, MEI is found to be relatively important.



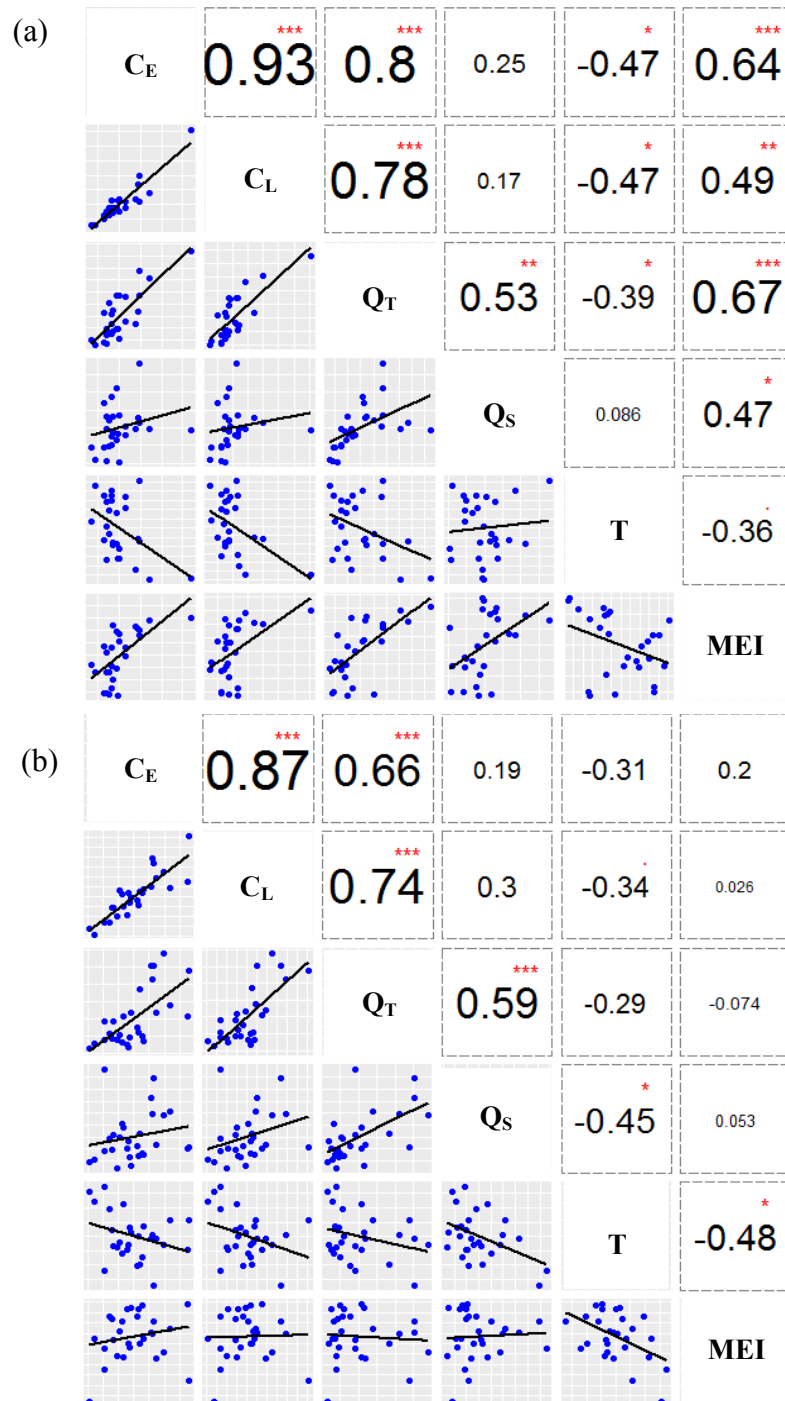
**Figure 4-10.** Relative Importance of Predictor Variables (discharge from the Trinity River, water temperature and MEI) in West Bay.

Table 4 summarizes all of the key factors identified through this process. It suggests that discharge is a key factor in Trinity, San Jacinto, East, and Lower Bays during most seasons. Trinity and San Jacinto Bays (which are close to the river outlets) are more affected by water temperature in OND and JFM, while East and Lower bays are also affected by MEI during JFM. West Bay is least affected by these factors, largely due to its various exchanges with the greater ocean.

**Table 4-1.** Significant driving factors of chla in each seasonal group ( $p < 0.01$ ).

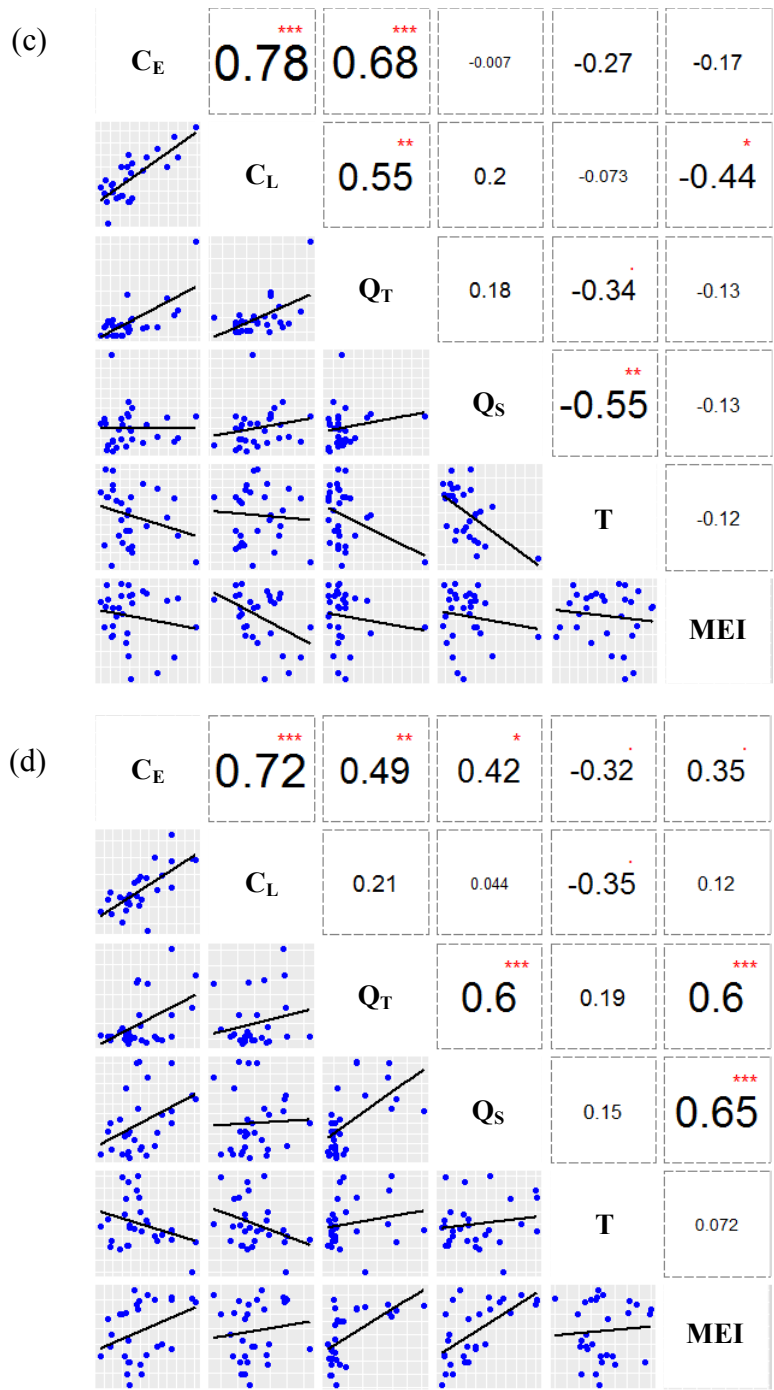
Segments	Significantly driving factors of chla ( $p < 0.01$ )			
	JFM	AMJ	JAS	OND
Trinity Bay	Q & T	Q	Q	T
San Jacinto Bay	Q & T	Q	Q	T
East Bay	Q & MEI	Q	Q	Q
Lower Bay	Q & MEI	Q	Q	T *
West Bay	Q & MEI	MEI *	NA	NA

\*  $p < 0.05$



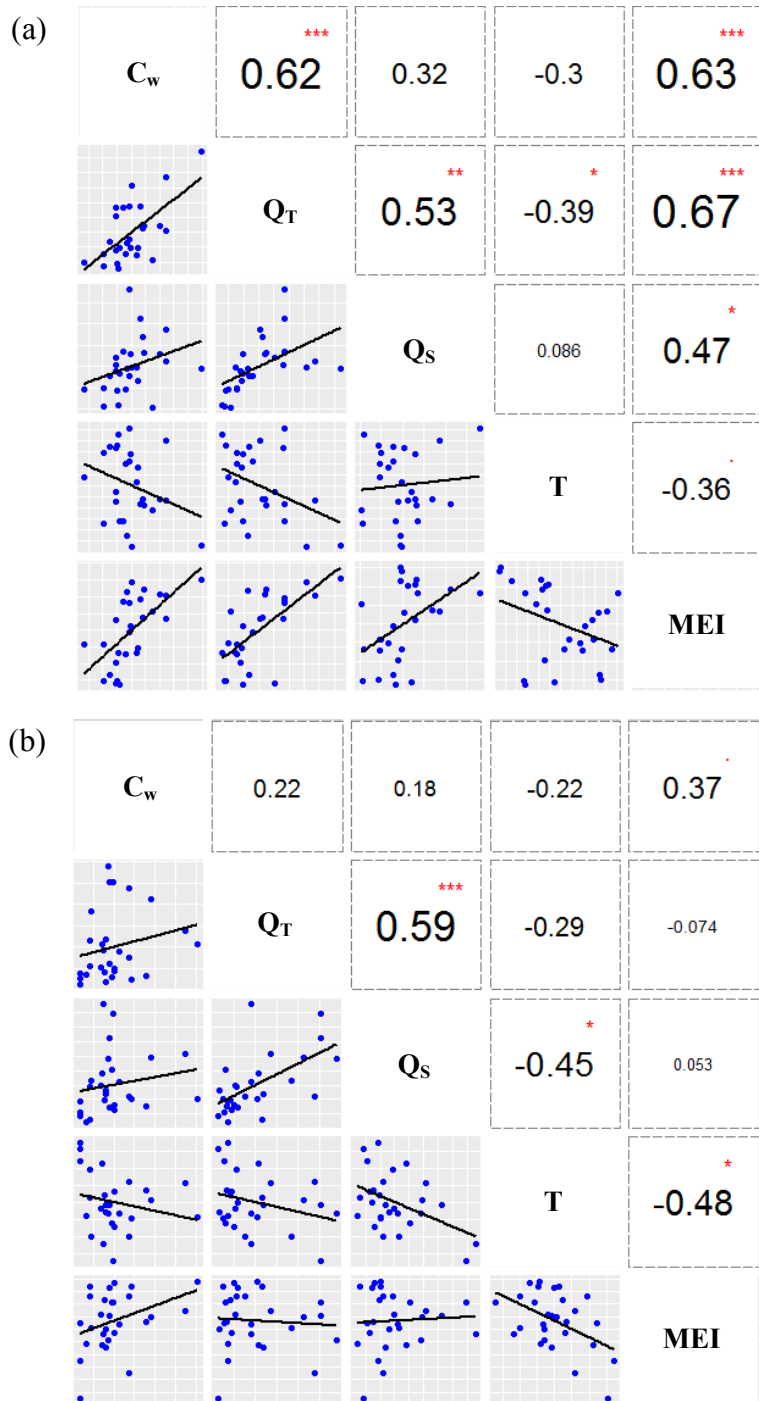
Significant codes:  $p < 0.001$  \*\*\*;  $0.001 < p < 0.01$  \*\*;  $0.01 < p < 0.05$  \*;  $0.01 < p < 0.1$

**Figure 4-11.** The monthly average correlation among  $C_E$  (chl<sub>a</sub> anomaly in the East Bay,  $\mu\text{g/L}$ ),  $C_L$  (chl<sub>a</sub> anomaly in the Lower Bay,  $\mu\text{g/L}$ ),  $T$  (water temperature anomaly,  $^{\circ}\text{C}$ ),  $MEI$  (Multiple ENSO Index from NOAA),  $Q_T$  (discharge anomaly from the Trinity River,  $\text{m}^3/\text{s}$ ) and  $Q_S$  (discharge anomaly from the San Jacinto River,  $\text{m}^3/\text{s}$ ) in (a) JFM; (b) AMJ; (c) JAS and (d) OND.



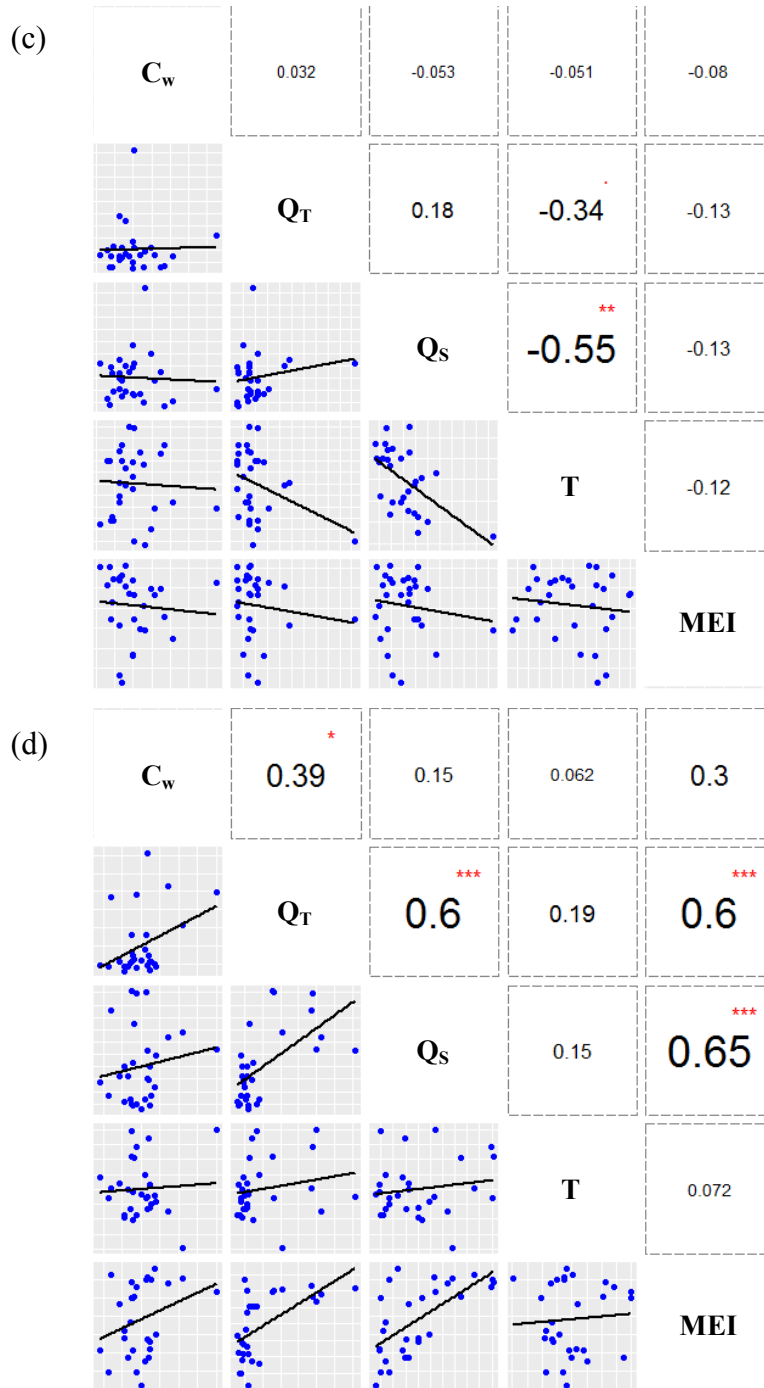
Significant codes:  $p < 0.001$  \*\*\*;  $0.001 < p < 0.01$  \*\*;  $0.01 < p < 0.05$  \*;  $0.01 < p < 0.1$  .

Figure 4-11. Continued.



Significant codes:  $p < 0.001$  \*\*\*;  $0.001 < p < 0.01$  \*\*;  $0.01 < p < 0.05$  \*;  $0.01 < p < 0.1$  .

**Figure 4-12.** The monthly average correlation among  $C_w$  (chl<sub>a</sub> anomaly in the West Bay,  $\mu\text{g/L}$ ),  $T$  (water temperature anomaly,  $^{\circ}\text{C}$ ),  $MEI$  (Multiple ENSO Index from NOAA),  $Q_T$  (discharge anomaly from the Trinity River,  $\text{m}^3/\text{s}$ ) and  $Q_S$  (discharge anomaly from the San Jacinto River,  $\text{m}^3/\text{s}$ ) in (a) JFM; (b) AMJ; (c) JAS and (d) OND.



Significant codes:  $p < 0.001$  \*\*\*;  $0.001 < p < 0.01$  \*\*;  $0.01 < p < 0.05$  \*;  $0.01 < p < 0.1$

Figure 4-12. Continued.

### 4.3 Chla Prediction Model

The environmental factors, including discharge, water temperature and MEI, are used to develop the chla prediction model. Considering the climatological impacts and seasonal variability, by removing the 10-year monthly average, the anomaly of chla, discharge and water temperature are used for model derivation in different seasonal groups. The coefficients in the prediction models are determined using the training dataset from May 2002 to December 2008. The predicted chla concentrations are evaluated against the observations during the testing period from January 2009 to December 2011. These statistic parameters used for testing the results are determination of coefficient  $R^2$ , mean absolute error (MAE) and root mean squared error (RMSE) (Equations (4-1) to (4-3)).

$$R^2 = 1 - \frac{\sum_{i=1}^n (x_i - y_i)^2}{\sum_{i=1}^n (x_i - \bar{x})^2} \quad (4-1)$$

$$MAE = \frac{\sum_{i=1}^n |y_i - x_i|}{n} \quad (4-2)$$

$$RMSE = \sqrt{\frac{\sum_{i=1}^n (y_i - x_i)^2}{n}} \quad (4-3)$$

where  $x_i$  is  $i^{th}$  the observation record;  $\bar{x}$  is the average of the observation data,  $y_i$  is the  $i^{th}$  predicted value from model, and n is number of the observation data.



#### 4.3.1 Trinity Bay and San Jacinto Bay

##### (1) Prediction model setup

Table 4-2 shows the linear regression models developed for Trinity Bay and San Jacinto Bay. The models are constructed using two variables: water temperature anomalies and the discharge anomalies of the Trinity River. A prediction model of the averaged chl<sub>a</sub> of the northern segment (Trinity Bay and San Jacinto Bay combined) is also developed, in which discharge from the San Jacinto River is included as well. This result is later compared with the results from two segments separately.

Both in Trinity Bay and San Jacinto Bay, the prediction models perform reasonably well in AMJ and JAS ( $p < 0.001$  and  $p < 0.05$ , respectively), indicating that chl<sub>a</sub> anomalies can be forecasted using the discharge anomalies from the Trinity River alone. However, in JFM, when spring algal blooming starts, the linear regression performance is not very significant ( $R^2 = 0.22$  in Trinity Bay and  $0.24$  in San Jacinto Bay). This suggests that just considering the influences from river discharge and water temperature – but excluding the other environmental factors such as nutrient concentration, solar radiation, salinity, or intense pollution events, etc. – would affect the accumulation of biomass during the spring and, in turn, cause uncertainties in chl<sub>a</sub> prediction. Furthermore, interactions between those factors and chl<sub>a</sub> could be more complicated than just the simple linear relationships. In OND, although the correlation is insignificant ( $R^2 = 0.11$ ) in Trinity Bay, the resulted MAE and RMSE are very small, indicating small biases from the prediction model. This means the prediction model in this

seasonal group can still produce acceptable results over Trinity Bay. In San Jacinto Bay, water temperature can be used for chla prediction with high significance ( $p < 0.05$ ), which is consistent with the correlation results in Figure 4-7 and Figure 4-8.

Table 4-2(c) shows the performance of the regression model over the entire northern segment containing inflow from the San Jacinto River. As compared to the results in Table 4-2(a) and (b), the prediction model performs well in JFM. This suggests that the within the chla prediction model, ignoring the San Jacinto inflow would add to the chla forecast error, especially in JFM.

**Table 4-2.** Prediction models developed in (a) Trinity Bay; (b) San Jacinto Bay; (c) Trinity Bay and San Jacinto Bay combined.

<b>(a)</b>					
Seasonal group	equation	$R^2$	MAE ( $\mu\text{g/L}$ )	RMSE ( $\mu\text{g/L}$ )	$p$ -value
<b>JFM</b>	$C_T = -0.439 + 0.005Q_T - 0.285T$	0.22	2.69	3.24	0.46
<b>AMJ</b>	$C_T = -0.389 + 0.014Q_T$	0.77	1.83	2.25	$<0.001^{***}$
<b>JAS</b>	$C_T = -0.273 + 0.006Q_T$	0.75	0.7	1.02	$<0.001^{***}$
<b>OND</b>	$C_T = -0.404 - 0.537T$	0.23	1.12	1.52	0.38

<b>(b)</b>					
Seasonal group	equation	$R^2$	MAE ( $\mu\text{g/L}$ )	RMSE ( $\mu\text{g/L}$ )	$p$ -value
<b>JFM</b>	$C_S = -0.084 + 0.007 Q_T - 0.438T$	0.24	2.57	3.46	0.26
<b>AMJ</b>	$C_S = 0.616 + 0.011Q_T$	0.56	2.36	3.25	$<0.01^{**}$

Table 4-2. Continued.

(b)

Seasonal group	equation	R <sup>2</sup>	MAE (µg/L)	RMSE (µg/L)	p-value
JAS	$C_S = 0.185 + 0.003Q_T$	0.38	0.91	1.29	<0.05*
OND	$C_S = -0.229 - 0.677T$	0.41	1.01	1.24	<0.05*

(c)

Seasonal group	equation	R <sup>2</sup>	MAE	RMSE	p-value
JFM	$C_{avg} = 0.107 + 0.014 Q_T - 0.040Q_S$	0.64	1.75	2.03	<0.01**
AMJ	$C_{avg} = -0.084 + 0.013Q_T$	0.73	1.97	2.33	<0.001***
JAS	$C_{avg} = -0.134 + 0.005Q_T$	0.75	0.71	0.95	<0.001***
OND	$C_{avg} = -0.351 - 0.580T$	0.29	1.09	1.40	0.10

**Significant codes:**  $p < 0.001$  \*\*\*;  $0.001 < p < 0.01$  \*\*;  $0.01 < p < 0.05$  \*;  $0.01 < p < 0.1$

Where  $C_T$  is chla anomaly in Trinity Bay;  $C_S$  is chla anomaly in San Jacinto Bay;  $C_{avg}$  is chla anomaly of the entire northern segment;  $Q_T$  is discharge anomaly for the Trinity River;  $Q_S$  is the discharge anomaly for the San Jacinto River; and  $T$  is water temperature anomaly.

## (2) Model validation

The prediction equations are validated using the testing dataset during the period of January 2009 – December 2011. The statistic results are shown in Table 4-3. For all four seasonal groups, the model validation results show the good predictable performance in Trinity Bay and San Jacinto Bay. For Trinity Bay, although the R<sup>2</sup> value is very low in

JAS, the model still shows acceptable skills with low MAE (0.92  $\mu\text{g/L}$ ) and RMSE (1.32  $\mu\text{g/L}$ ). For the whole northern segment, all of the statistic values indicate the prediction model performs better than the models generated over an individual segment (Trinity or San Jacinto).

**Table 4-3.** Prediction model tested over Trinity Bay and San Jacinto Bay.

Seasonal group	Trinity Bay			San Jacinto Bay			Whole northern segment		
	R <sup>2</sup>	MAE ( $\mu\text{g/L}$ )	RMSE ( $\mu\text{g/L}$ )	R <sup>2</sup>	MAE ( $\mu\text{g/L}$ )	RMSE ( $\mu\text{g/L}$ )	R <sup>2</sup>	MAE ( $\mu\text{g/L}$ )	RMSE ( $\mu\text{g/L}$ )
<b>JFM</b>	0.74	3.95	5.33	0.80	2.47	3.35	0.74	3.16	3.58
<b>AMJ</b>	0.45	3.07	3.89	0.43	2.53	2.99	0.46	2.52	3.14
<b>JAS</b>	0	0.92	1.32	0	1.38	1.50	0	0.77	1.15
<b>OND</b>	0.18	1.62	1.90	0.54	0.84	1.04	0.27	1.33	1.57
<b>All</b>	0.59	2.39	3.50	0.59	1.80	2.42	0.66	1.94	2.57

Figure 4-13 suggests that the prediction models performance well in both Trinity Bay ( $R^2 = 0.60$ ) and San Jacinto Bay ( $R^2 = 0.61$ ). The models, however, do have a tendency of underestimating the peak values, especially in the wet years (e.g., 2003, 2007, 2008, 2009 and 2010). Those peaks of chla concentrations usually occur between March and May, such as in May 2009 and March 2010. In constructing the models, discharge from the Trinity River is employed as the primary inflow driving the chla variations, both in Trinity Bay and San Jacinto Bay. However, even though the influence of discharge from the San Jacinto River is found relatively insignificant on regulating chla concentrations in

each of the two northern segments, the analysis of the whole northern segment (Table 4.2) indicates that ignoring the discharge from San Jacinto River in the prediction model leads to less robust results.

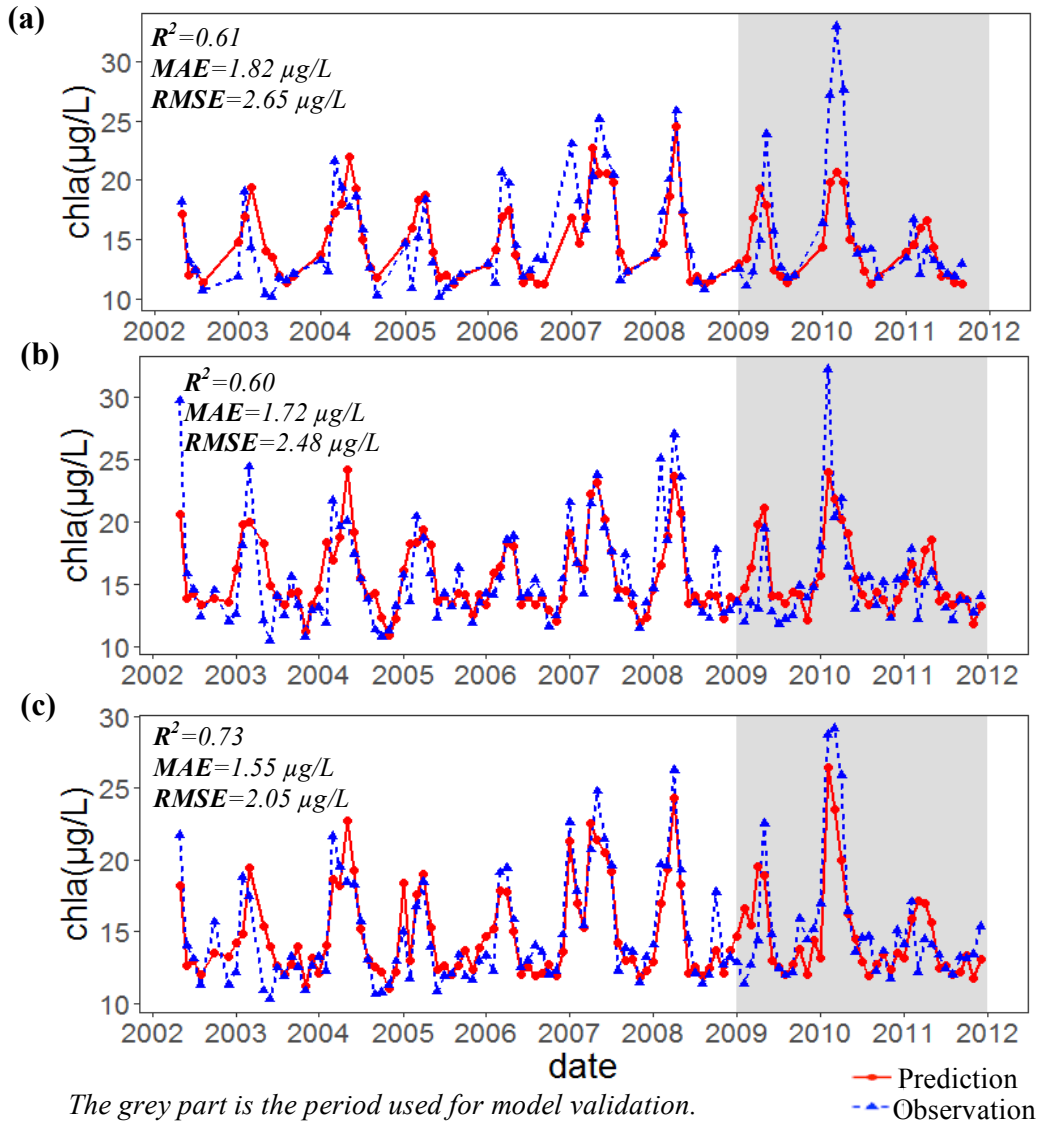


**Figure 4-13.** Model prediction results (red) and observation (blue) in (a) Trinity Bay; (b) San Jacinto Bay; (c) the whole northern segment (the shading indicates the testing period).

### 4.3.2 East Bay and Lower Bay

#### (1) Prediction model setup

The approach as described in 4.3 is applied to East Bay and Lower Bay for developing the prediction models. As shown in Figure 4-4, high correlations of the chl<sub>a</sub> concentrations are found between these two segments, between East Bay and Trinity Bay, as well as between Lower Bay and San Jacinto Bay. Thus, even these two segments are neither directly connected to the Trinity River nor the San Jacinto River, their chl<sub>a</sub> concentrations are still much affected by the freshwater loading from these two major rivers.

The results in Table 4-4 show that chl<sub>a</sub> anomalies can be predicted well both in East Bay and Lower Bay using discharge anomalies from the Trinity River alone in all seasons except for OND.

**Table 4-4.** Prediction models developed in (a) East Bay; (b) Lower Bay.

<b>(a)</b>					
Seasonal group	equation	R <sup>2</sup>	MAE (µg/L)	RMSE (µg/L)	p-value
<b>JFM</b>	$C_E = -0.728 + 0.010Q_T$	0.39	1.91	2.31	<0.01**
<b>AMJ</b>	$C_E = -0.037 + 0.006Q_T$	0.78	1.01	1.22	<0.001***
<b>JAS</b>	$C_E = -0.105 + 0.004Q_T$	0.50	0.80	0.98	<0.001***
<b>OND</b>	$C_E = -0.662 - 0.001 Q_T$	0.22	0.81	1.01	0.46

**Table 4-4.** Continued.**(b)**

Seasonal group	equation	R <sup>2</sup>	MAE (µg/L)	RMSE (µg/L)	p-value
<b>JFM</b>	$C_L = -0.869 + 0.013Q_T$	0.34	2.44	3.00	<0.01**
<b>AMJ</b>	$C_L = -0.318 + 0.007Q_T$	0.68	1.34	1.55	<0.001***
<b>JAS</b>	$C_L = -0.029 + 0.002Q_T$	0.46	0.56	0.74	<0.01**
<b>OND</b>	$C_L = -0.080 - 0.356T$	0.24	2.13	2.68	0.25

*Significant codes:  $p < 0.001$  \*\*\*;  $0.001 < p < 0.01$  \*\*;  $0.01 < p < 0.05$  \*;  $0.01 < p < 0.1$*

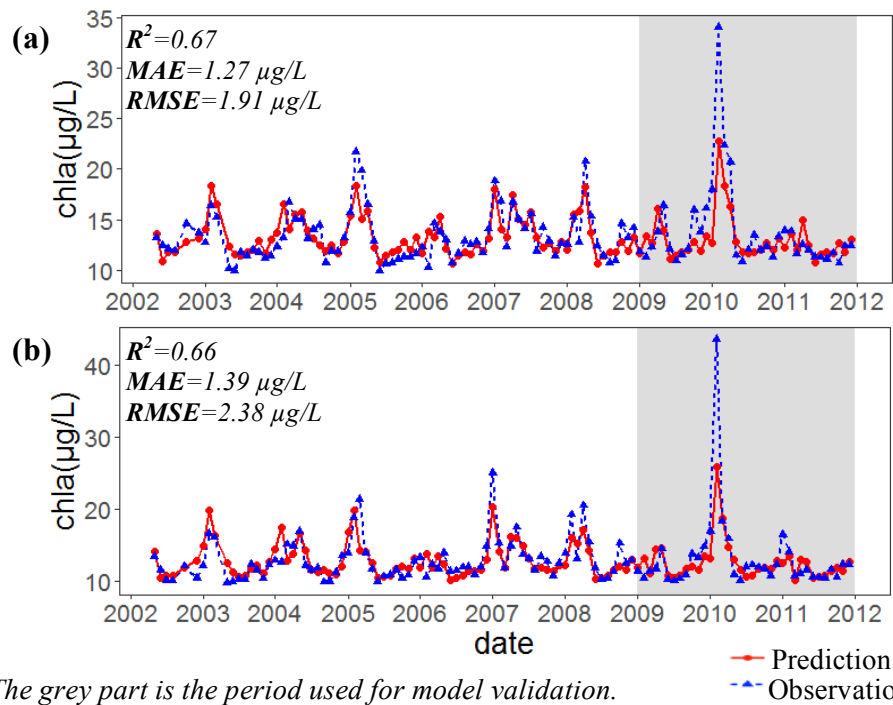
Where  $C_E$  is the chla anomaly of East Bay;  $C_L$  is the chla anomaly of Lower Bay.

## (2) Model validation

The model validation results in East Bay and Lower Bay are provided in Table 4-5. Considering the four seasonal groups, all R<sup>2</sup>, MAE and RMSE values indicate the robust performance of the prediction model. Similarly, in Figure 4-14, the predicted chla time series agree well with the observations. Still, the prediction model has some weakness in accurately representing the peak chla values (especially in 2005, 2007, 2008 and 2010).

**Table 4-5.** Prediction model tested over East Bay and Lower Bay.

Seasonal group	East Bay			Lower Bay		
	R <sup>2</sup>	MAE (µg/L)	RMSE (µg/L)	R <sup>2</sup>	MAE (µg/L)	RMSE (µg/L)
<b>JFM</b>	0.90	2.82	4.44	0.88	3.40	6.26
<b>AMJ</b>	0.51	1.74	2.11	0.60	1.28	1.55
<b>JAS</b>	0.13	0.44	0.66	0.12	0.61	0.76
<b>OND</b>	0.42	1.50	1.72	0.27	1.00	1.13
<b>All</b>	0.80	1.59	2.63	0.82	1.57	3.30



The grey part is the period used for model validation.

**Figure 4-14.** Model prediction results (red) and observations (blue) in (a) East Bay; (b) Lower Bay (the shading indicates the testing period).



### 4.3.3 West Bay

#### (1) Prediction model setup

Compared with other segments, West Bay has the lowest chl<sub>a</sub> concentrations with little variations over the 10-year period. Using the same approach, the prediction model is developed in West Bay. Table 4-6 shows that the only the prediction equation for JFM can pass the significance test. Chl<sub>a</sub> in this segment can be predicted by MEI alone, which indicates the strong influence of climatological variability and El Niño Southern Oscillation (ENSO) on chl<sub>a</sub> in West Bay. In JAS and OND, chl<sub>a</sub> anomalies are constant values. It shows that in those two seasonal groups, the chl<sub>a</sub> anomalies are insensitive to any of the environmental drivers selected in this study. Thus, chl<sub>a</sub> concentrations in JAS and OND are dominated by the seasonal climatology.

**Table 4-6.** Prediction models developed in West Bay.

Seasonal group	equation	R <sup>2</sup>	MAE (µg/L)	RMSE (µg/L)	p-value
<b>JFM</b>	$C_W = -0.132 + 1.156MEI$	0.57	0.94	1.18	<0.01**
<b>AMJ</b>	$C_W = -0.166 + 0.259MEI$	0.13	0.70	0.92	0.59
<b>JAS</b>	$C_W = 0.0004$	0.04	0.47	0.68	
<b>OND</b>	$C_W = 0.0008$	0.65	0.79	1.13	

*Significant codes:  $p < 0.001$  \*\*\*;  $0.001 < p < 0.01$  \*\*;  $0.01 < p < 0.05$  \*;  $0.01 < p < 0.1$*

Where  $C_W$  is the chl<sub>a</sub> anomaly of West Bay.

(2) Model validation

The model validation results in West Bay are shown in Table 4-7 and Figure 4-15. Even with the relatively low  $R^2$ , considering the lower MAE (0.99  $\mu\text{g/L}$ ) and RMSE (1.40  $\mu\text{g/L}$ ), the prediction model performs reasonably as well. However, similar deficiency of model prediction ability is observed in representing annual peak values of chl<sub>a</sub>. Thus, during the wet year, more environmental factors need to be considered to develop prediction models for predicting severe events, such as harmful algal blooms (HABs).

**Table 4-7.** Prediction equation tested over West Bay.

Seasonal group	$R^2$	MAE ( $\mu\text{g/L}$ )	RMSE ( $\mu\text{g/L}$ )
JFM	0.56	1.15	1.49
AMJ	0.33	1.34	1.91
JAS	0.02	0.47	0.57
OND	0.35	1.01	1.30
All	0.47	0.99	1.40

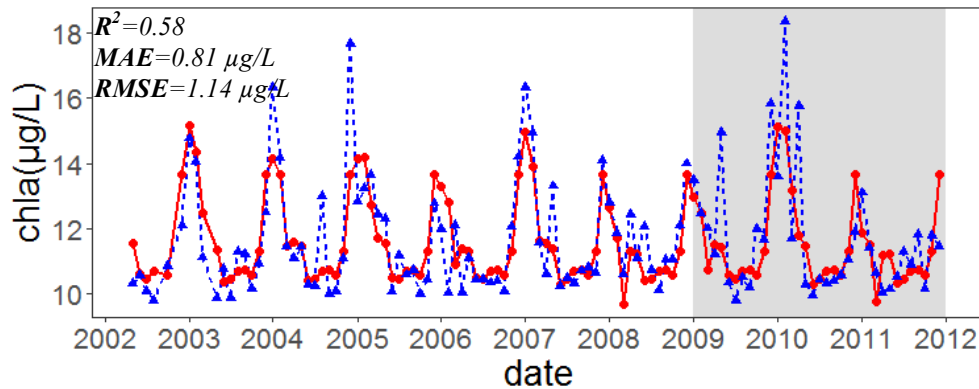


**Figure 4-15.** Model prediction results (red) and observation (blue) in the West Bay (the shading indicates the testing period).

#### 4.3.4 Relationship between air temperature and water temperature

Because water temperature is difficult to model, we used an empirical regression method to estimate the water temperature from the climate model forecasted air temperature. The linear relationship between the air and water temperature was developed using observation data (Figure 4-16). Hourly water temperature data was acquired from the Texas Water Development Board (TWDB) and hourly air temperature data was also collected by NOAA. In both cases, observations were averaged to monthly value to develop the relationship shown in Figure 4-16. This regression equation provides the feasibility for chl a prediction by using air temperature, even when water temperature data is lacking.

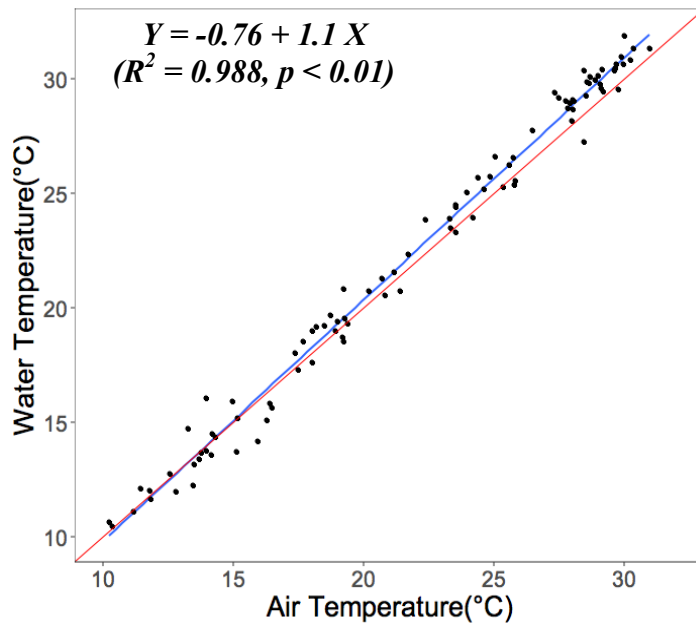


**Figure 4-16.** Linear regression relationship between air temperature and water temperature.

## 5. DISCUSSION

The spatial distributions of chl<sub>a</sub> concentrations in Galveston Bay show relatively higher values in the northern segments compared with the southern segments in different locations. This finding is similar with research conducted in other bays, such as the Chesapeake Bay (Harding *et al.* 2016) and Pensacola Bay (Le *et al.* 2016). In addition, the positive response of chl<sub>a</sub> to discharge is consistent with research results shown in other bay areas, which indicates the significant influence of discharge from inland on algal growth. Low chl<sub>a</sub> concentration in West Bay indicates that in the parts of the bay linked to sea, high salt content will restrain the growth of algae.

The study by Roelke *et al.* (2013) using *in situ* data showed that correlation performances between chl<sub>a</sub> concentration and discharge from rivers were different in Trinity Bay and San Jacinto Bay. The discharge from the Trinity River had negative influence on chl<sub>a</sub> in Trinity Bay. Positive influence was observed between discharge of the San Jacinto River and chl<sub>a</sub> in San Jacinto Bay. However, in this study by using chl<sub>a</sub> derived from remote sensing data, it suggests that chl<sub>a</sub> in both San Jacinto Bay and Trinity Bay have positive correlations with discharge from the Trinity River. Different datasets with different spatial and temporal resolutions were analyzed in these two studies. A single point and one monitoring data per month for each of these segments is used in Roelke *et al.* (2013), but in this study, the dataset with 3-day records for around 260m × 300m spatial resolution of the whole bay are used and the value of all cells within these segments are averaged and analyzed. At the same time, research time periods with over 10 years are

different with the research from Roelke *et al.* (2013) (two years of 2005 and 2006 are explored), which will contribute to the different results.

Small errors can be introduced to the chl<sub>a</sub> prediction model when the water temperature time series are a result of data from multiple locations. At different monitoring stations, water temperature are slightly different (Figure A-2 in Appendix A). When temperature data borrowed from other stations, the predictions of chl<sub>a</sub> can be biased, especially in JFM and OND. The error introduced by 1 °C difference ranges from -0.677 µg/L (4.4%) in San Jacinto Bay to -0.148 µg/L (1.1%) in OND, which is larger than the error in JFM (maximum is -0.438 µg/L in San Jacinto Bay).

Moreover, unlike the results shown in Tampa Bay in Florida (Le *et al.* 2013) where positive correlation exists between chl<sub>a</sub> and MEI, no significant correlation is observed between the two in Galveston Bay (except for JFM in West Bay). Directly connected with Gulf of Mexico, West Bay is more affected by climatological variation (e.g., ENSO). Thus, based on MEI, chl<sub>a</sub> can be predicted in this segment.

This research focuses solely on freshwater inflow volume and climatic factors (mainly water temperature and MEI). However, other elements can contribute to chl<sub>a</sub> concentration variations as well, such as water quality parameters (like phosphorus and nitrogen), the hydrodynamic condition, solar radiation and sediment transportation. In addition, biological processes – including the overall food chain (e.g. grazing by zooplankton, filtration by shellfish, etc.), and the growth cycle of algae – may also affect the chl<sub>a</sub> concentration level. Without considering those complicated causes of chl<sub>a</sub> variability and mechanical physical-chemical-biological processes, uncertainties for chl<sub>a</sub>

prediction will be introduced in this research. Therefore, challenges still exist for developing a more comprehensive understanding about the interactions between chl<sub>a</sub> and environmental factors. Thus, by combining with mechanism model with data-driven approaches to consider the physical-chemical-biological processes, the models for chl<sub>a</sub> prediction would be more profound and meaningful for eco-environmental management in Galveston Bay and other estuary region.

## 6. CONCLUSIONS

As the seventh largest estuaries in the U.S., Galveston Bay has significant ecological, economic and recreational values for the State of Texas. The objectives of this study are to identify the spatial-temporal variations of chl<sub>a</sub>, and to investigate the impacts of freshwater inflow and climatic factors on chl<sub>a</sub> variability – so that prediction models can be developed for chl<sub>a</sub> forecasting in Galveston Bay.

A 10-year validated remote sensing dataset are used to study the spatial-temporal variations of chl<sub>a</sub> concentrations in Galveston Bay. Three environmental factors – discharges from the Trinity River and the San Jacinto River, water temperature, and MEI – are chosen to explore their interactions with chl<sub>a</sub> concentrations over different segments and during different seasons. Using the key drivers identified, the prediction models are developed in the five segments. The results show that:

(1) The spatial distributions of chl<sub>a</sub> concentrations have shown clear patterns in Galveston Bay. Spatially, the chl<sub>a</sub> concentrations are low near the river outlet and round the Houston ship Channel (HSC). Otherwise, the chl<sub>a</sub> concentrations near the shoreline are typically higher than that in the center of the bay. In addition, chl<sub>a</sub> in the northern segments has the higher value than the southern parts. The highest value usually occurs in San Jacinto Bay, followed by Trinity Bay, East Bay, Lower Bay and West Bay.

(2) Temporally, the inter-annual variabilities of chl<sub>a</sub> are related to hydrological year by locations. Over the 10-year study period (from 2002 to 2011), the highest chl<sub>a</sub> concentration is found in the wettest year (2010), followed by a sharp decrease in extreme



drought year (2011). The seasonal fluctuations of chl<sub>a</sub> are higher during the wet months (from February to May) compared with the other months (especially from August to December). Both annual and inter-annual variations in the northern segments are greater than the southern segments.

(3) After eliminating the seasonal variations from the chl<sub>a</sub> concentrations and the environmental factors, correlation analysis results suggest that discharge anomalies have positive effects on chl<sub>a</sub> anomalies, while water temperature anomalies exhibit negative effects. The key driving factors of chl<sub>a</sub> vary in different seasonal groups. For the whole bay area (except for West Bay), chl<sub>a</sub> is primarily determined by discharge from the Trinity River in AMJ and JAS. However, in OND, the main driving factor is water temperature. In JFM, all of the factors (except for the discharge from the San Jacinto River) show significant correlations with chl<sub>a</sub> concentrations. Additionally, correlation relations also exist among those factors themselves.

(4) Chl<sub>a</sub> prediction models are developed based on correlation analysis, multiple linear regression and stepwise regression. Overall, the prediction models have performed well in different segments and seasonal groups ( $0.58 < R^2 < 0.73$ ,  $0.81 \mu\text{g/L} < \text{MAE} < 1.82 \mu\text{g/L}$ ,  $1.14 \mu\text{g/L} < \text{RMSE} < 2.65 \mu\text{g/L}$ ). However, those models are still limited in predicting the annual peak value of chl<sub>a</sub> (also see Appendix B). Thus, other factors – such as nutrients, solar radiation, salinity, intense pollution events – may have played considerable roles in stimulating extreme events (e.g. HABs).

In general, this research provides a comprehensive understanding on interactions between chl<sub>a</sub> concentrations and a set of key environment factors. Quantitative prediction

models of chl<sub>a</sub> are developed and tested for Galveston Bay. The advantages of using a remotely sensed long-term chl<sub>a</sub> dataset are fully demonstrated. The results can provide scientific guide for coastal environmental management, maintaining the eco-environmental health and reducing eutrophication risk in the future in Galveston Bay.

## REFERENCES

- Armstrong, N. E. and Ward Jr, G. H. (1993). Point source loading characterization of Galveston Bay. Galveston Bay National Estuary Program.
- Barnes, R.A., Holmes, A.W. and Esalas, W.E. (1995), Stray Light in the SeaWiFS Radiometer SeaWiFS Technical Report Series, vol. 31. NASA Technical Memorandum 104566, 76.
- Bricker, S. B., B. Longstaf, W. Dennison, A. Jones, K. Boicourt, C. Wicks and J. Woerner (2008). Effects of nutrient enrichment in the nation's estuaries: A decade of change. *Harmful Algae* 8(1): 21-32.
- Buskey, E. and Schmidt, K. (1992). Characterization of plankton from the Galveston estuary. Status and Trends of Selected Living Resources in the Galveston Bay System. Galveston Bay National Estuary Program Publication GBNEP-19. The Galveston Bay National Estuary Program, Webster, 347-375.
- Buyukates, Y. and Roelke, D. (2005). Influence of pulsed inflows and nutrient loading on zooplankton and phytoplankton community structure and biomass in microcosm experiments using estuarine assemblages. *Hydrobiologia* 548(1): 233-249.
- Camacho, R. A., J. L. Martin, B. Watson, M. J. Paul, L. Zheng and J. B. Stribling (2015). Modeling the Factors Controlling Phytoplankton in the St. Louis Bay Estuary, Mississippi and Evaluating Estuarine Responses to Nutrient Load Modifications. *Journal of Environmental Engineering* 141(3).

- Chavez, F. P., P. G. Strutton, C. E. Friederich, R. A. Feely, G. C. Feldman, D. C. Foley and M. J. McPhaden (1999). Biological and chemical response of the equatorial Pacific Ocean to the 1997-98 El Nino. *Science* 286(5447): 2126-2131.
- Cloern, J. E. (1991). Tidal stirring and phytoplankton bloom dynamics in an estuary. *Journal of marine research* 49(1): 203-221.
- Cloern, J. E. (2001). Our evolving conceptual model of the coastal eutrophication problem. *Marine Ecology Progress Series* 210: 223-253.
- Cloern, J. E., N. Knowles, L. R. Brown, D. Cayan, M. D. Dettinger, T. L. Morgan, D. H. Schoellhamer, M. T. Stacey, M. van der Wegen, R. W. Wagner and A. D. Jassby (2011). Projected Evolution of California's San Francisco Bay-Delta-River System in a Century of Climate Change. *Plos One* 6(9).
- Derksen, S. and Keselman, H. J. (1992). Backward, forward and stepwise automated subset selection algorithms: Frequency of obtaining authentic and noise variables. *British Journal of Mathematical and Statistical Psychology* 45(2): 265-282.
- Dorado, S., T. Booe, J. Steichen, A. S. McInnes, R. Windham, A. Shepard, A. E. B. Lucchese, H. Preischel, J. L. Pinckney, S. E. Davis, D. L. Roelke and A. Quigg (2015). Towards an Understanding of the Interactions between Freshwater Inflows and Phytoplankton Communities in a Subtropical Estuary in the Gulf of Mexico. *Plos One* 10(7).
- Dos Santos, A. C. A., Calijuri, M. D. C., Moraes, E. M., Adorno, M. A. T., Falco, P. B., Carvalho, D. P. and Benassi, S. F. (2003). Comparison of three methods for Chlorophyll determination: Spectrophotometry and Fluorimetry in samples

containing pigment mixtures and spectrophotometry in samples with separate pigments through High Performance Liquid Chromatography. *Acta Limnol. Bras* 15(3): 7-18.

Drake, P., A. M. Arias, F. Baldo, J. A. Cuesta, A. Rodriguez, A. Silva-Garcia, I. Sobrino, D. Garcia-Gonzalez and C. Fernandez-Delgado (2002). Spatial and temporal variation of the nekton and hyperbenthos from a temperate European estuary with regulated freshwater inflow. *Estuaries* 25(3): 451-468.

Dzwonkowski, B., Yan, X. H. (2005). Development and application of a neural network based ocean colour algorithm in coastal waters. *International Journal of Remote Sensing* 26(6): 1175-1200.

Froneman, P. W. (2002). Response of the plankton to three different hydrological phases of the temporarily open/closed Kasouga estuary, South Africa. *Estuarine Coastal and Shelf Science* 55(4): 535-546.

Galveston Bay Report Card, 2015. [http://www.galvbaygrade.org/wp-content/uploads/2015/07/Galveston\\_Bay\\_Full\\_Report\\_updweb.pdf](http://www.galvbaygrade.org/wp-content/uploads/2015/07/Galveston_Bay_Full_Report_updweb.pdf)

Grömping, U. (2006). Relative importance for linear regression in R: the package relaimpo. *Journal of statistical software* 17(1): 1-27.

Guannel, G., Guerry, A. D., Brenner, J., Faries, J., Thompson, M., Silver, J. and Verutes, G. (2014). Changes in the delivery of ecosystem services in Galveston Bay, TX, under a sea-level rise scenario. Palo Alto, CA.

- Han, L. and Jordan, K. J. (2005). Estimating and mapping chlorophyll-a concentration in Pensacola Bay, Florida using Landsat ETM+ data. *International Journal of Remote Sensing* 26(23): 5245-5254.
- Harding, L. W. (1994). Long-Term Trends in the Distribution of Phytoplankton in Chesapeake Bay - Roles of Light, Nutrients and Streamflow. *Marine Ecology Progress Series* 104(3): 267-291.
- Harding, L. W., Jr., M. E. Mallonee, E. S. Perry, W. D. Miller, J. E. Adolf, C. L. Gallegos and H. W. Paerl (2016). Variable climatic conditions dominate recent phytoplankton dynamics in Chesapeake Bay. *Sci Rep* 6: 23773.
- Harding, L. W., A. Magnuson and M. E. Mallonee (2005). SeaWiFS retrievals of chlorophyll in Chesapeake Bay and the mid-Atlantic bight. *Estuarine Coastal and Shelf Science* 62(1-2): 75-94.
- Harding Jr. L. W., C. L. G., E. S. Perry, W. D. Miller, J. E. Adolf & M. E. Mallonee, H. W. Paerl (2016). Long-Term Trends of Nutrients and Phytoplankton in Chesapeake Bay. *Estuaries and Coasts* 39: 664–681.
- Jiang, J., Wang, P., Tian, Z., Guo, L., Wang, Y. (2011). A comparative study of statistical learning methods to predict eutrophication tendency in a reservoir, northeast China. In *Mechanic Automation and Control Engineering (MACE)*, 2011 Second International Conference on (pp. 1883-1886). IEEE.
- Johnson, J. W. (2000). A heuristic method for estimating the relative weight of predictor variables in multiple regression. *Multivariate behavioral research* 35(1): 1-19.

- Korosov, A. D., Pozdnyakov, D. V., Shuchman, R. A., Sayers, M. J. and Sawtell, R. W. (2015). Bio-optical retrieval algorithm for the optically shallow waters of the Great Lakes.
- Le, C., J. C. Lehrter, B. A. Schaeffer, C. Hu, M. C. Murrell, J. D. Hagy, R. M. Greene and M. Beck (2016). Bio-optical water quality dynamics observed from MERIS in Pensacola Bay, Florida. *Estuarine, Coastal and Shelf Science* 173: 26-38.
- Le, C., Hu, C., English, D., Cannizzaro, J. and Kovach, C. (2013). Climate-driven chlorophyll-a changes in a turbid estuary: Observations from satellites and implications for management. *Remote Sensing of Environment*.
- Liu, X. H., Y. L. Zhang, K. Shi, Y. Q. Zhou, X. M. Tang, G. W. Zhu and B. Q. Qin (2015). Mapping Aquatic Vegetation in a Large, Shallow Eutrophic Lake: A Frequency-Based Approach Using Multiple Years of MODIS Data. *Remote Sensing* 7(8): 10295-10320.
- Malone, T. C., L. H. Crocker, S. E. Pike and B. W. Wendler (1988). Influences of River Flow on the Dynamics of Phytoplankton Production in a Partially Stratified Estuary. *Marine Ecology Progress Series* 48(3): 235-249.
- Meybeck, M., G. Cauwet, S. Dessery, M. Somville, D. Gouleau and G. Billen (1988). Nutrients (Organic C, P, N, Si) in the Eutrophic River Loire (France) and Its Estuary. *Estuarine Coastal and Shelf Science* 27(6): 595-624.
- Miller, W. D. and L. W. Harding (2007). Climate forcing of the spring bloom in Chesapeake Bay. *Marine Ecology Progress Series* 331: 11-22.

- Örnólfssdóttir, E. B., Lumsden, S. E., & Pinckney, J. L. (2004). Phytoplankton community growth-rate response to nutrient pulses in a shallow turbid estuary, Galveston Bay, Texas. *Journal of plankton research* 26(3): 325-339.
- Örnólfssdóttir, E. B., S. E. Lumsden and J. L. Pinckney (2004). Nutrient pulsing as a regulator of phytoplankton abundance and community composition in Galveston Bay, Texas. *Journal of Experimental Marine Biology and Ecology* 303(2): 197-220.
- Rheuban, J. E., S. Williamson, J. E. Costa, D. M. Glover, R. W. Jakuba, D. C. McCorkle, C. Neill, T. Williams and S. C. Doney (2016). Spatial and temporal trends in summertime climate and water quality indicators in the coastal embayments of Buzzards Bay, Massachusetts. *Biogeosciences* 13(1): 253-265.
- Roberts, A. D. and S. D. Prince (2010). Effects of urban and non-urban land cover on nitrogen and phosphorus runoff to Chesapeake Bay. *Ecological Indicators* 10(2): 459-474.
- Roelke, D. L., H. P. Li, N. J. Hayden, C. J. Miller, S. E. Davis, A. Quigg and Y. Buyukates (2013). Co-occurring and opposing freshwater inflow effects on phytoplankton biomass, productivity and community composition of Galveston Bay, USA. *Marine Ecology Progress Series* 477: 61-76.
- Sathyendranath, S., L. Watts, E. Devred, T. Platt, C. Caverhill and H. Maass (2004). Discrimination of diatoms from other phytoplankton using ocean-colour data. *Marine Ecology Progress Series* 272: 59-68.



- Shen X., Gao H., Zhao G., Zhang S. (2016). The potential impact of freshwater inflows on Chlorophyll a in a shallow estuary: a case study in Galveston Bay, Texas. Poster, Asia Oceania Geosciences Society, Ocean Science Session, July 2016.
- Stenseth, N. C., A. Mysterud, G. Ottersen, J. W. Hurrell, K. S. Chan and M. Lima (2002). Ecological effects of climate fluctuations. *Science* 297(5585): 1292-1296.
- Tonidandel, S. and LeBreton, J. M. (2011). Relative importance analysis: A useful supplement to regression analysis. *Journal of Business and Psychology* 26(1): 1-9.
- Xia, M. and L. Jiang (2015). Influence of wind and river discharge on the hypoxia in a shallow bay. *Ocean Dynamics* 65(5): 665-678.
- Zhang, S., H. L. Gao, A. Quigg and D. L. Roelke (2016). Remote Sensing of Spatial-Temporal Variations of Chlorophyll-a in Galveston Bay, Texas. 2016 Ieee International Geoscience and Remote Sensing Symposium (Igarss): 5841-5844.

APPENDIX A

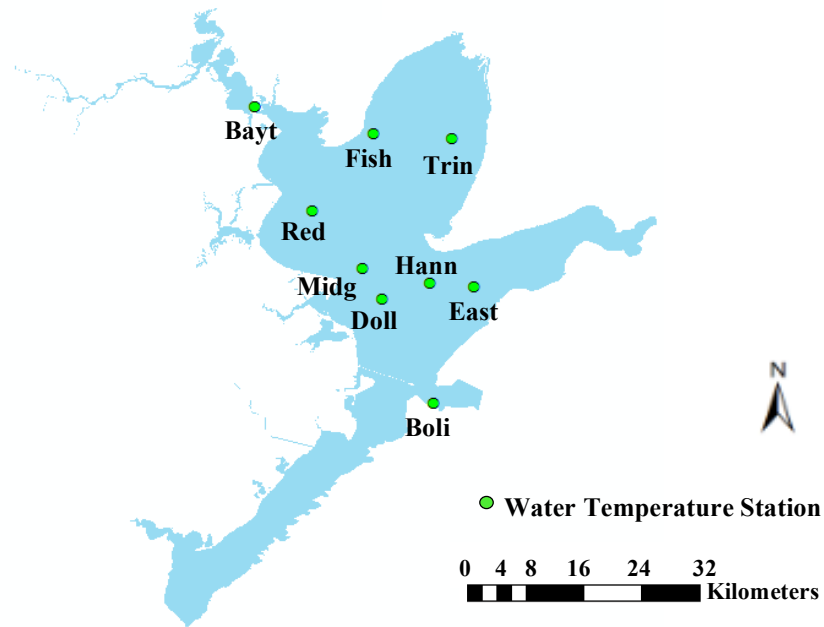


**Figure A-1** Water temperature monitoring station in Galveston Bay from Texas Water Development Board (TWDB)

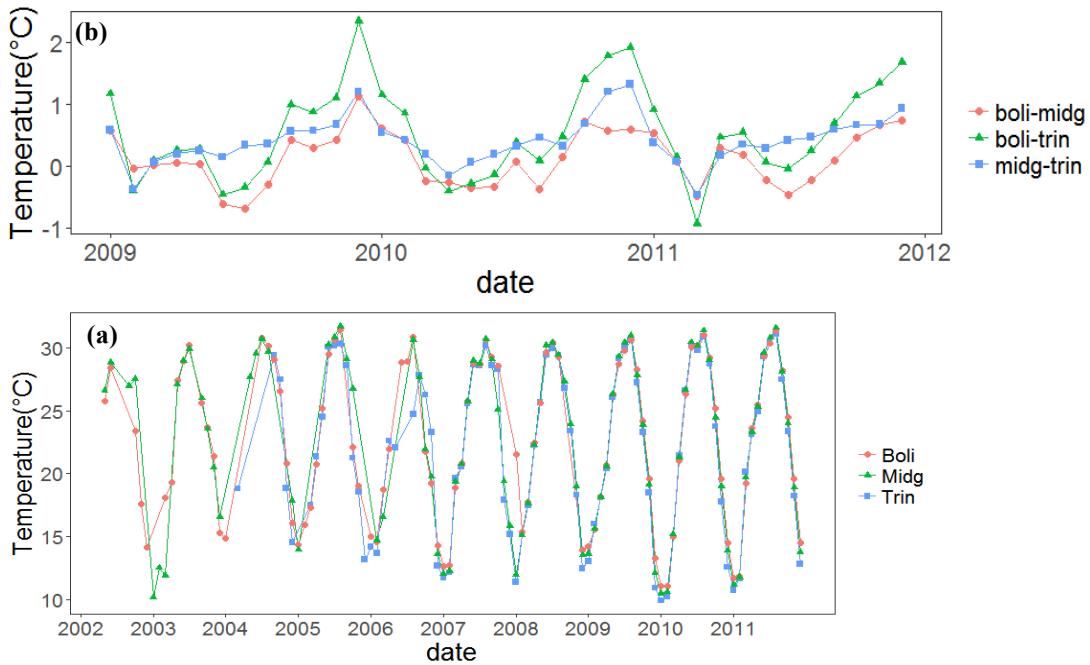


**Figure A-2** (a) Monthly water temperature time series from May 2002 to December 2012 (b) The water temperature differences among three monitoring station from 2009 to 2011.

To identify the uncertainties/errors associated with the use of water temperature from multiple stations, the water temperature differences among those three stations are compared with each other in A-2(b). It shows that usually, from June to August, water temperature in northern part is higher than the lower part ( $\text{Trin} > \text{Midg} > \text{Boli}$ ). In contrast, from October to February of the next year, water temperature shows the lower parts have higher values than the northern parts ( $\text{Boli} > \text{Midg} > \text{Trin}$ ). The largest difference occurs between Boli station and Trin station. However, even there is the water temperature difference existing, its range is among  $-1\text{ }^{\circ}\text{C} \sim 2\text{ }^{\circ}\text{C}$ . Because it is difficult to obtain the completed water temperature data all from one monitoring station. Data from other stations nearby are used to fill in the missing data to complete analysis. In this study, temperature in Boli is used for analysis and data from Midg is borrowed to fill in the missing values.

APPENDIX B

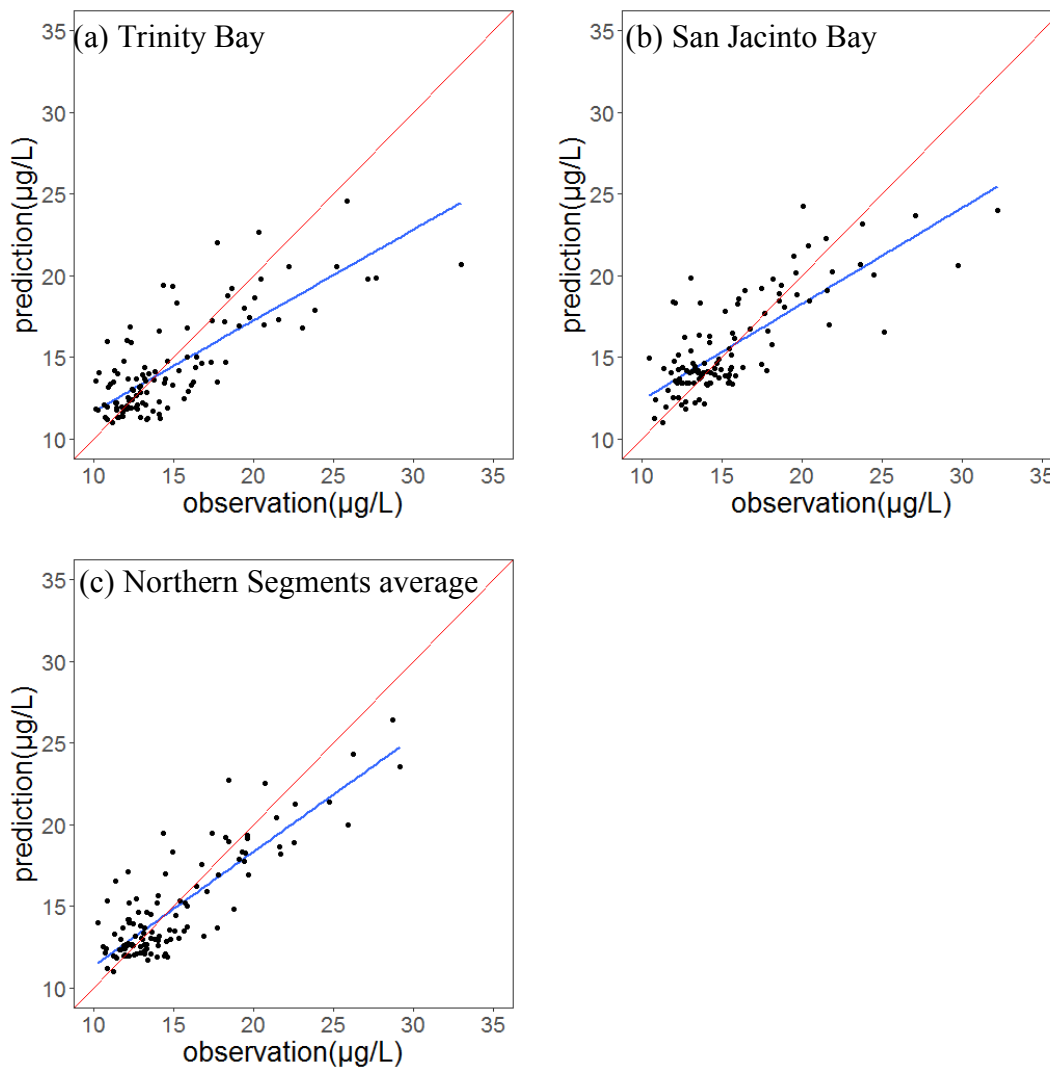


**Figure B-1** Comparison between prediction and observation chl a in (a) Trinity Bay, (b) San Jacinto Bay and (c) Northern Segments average.

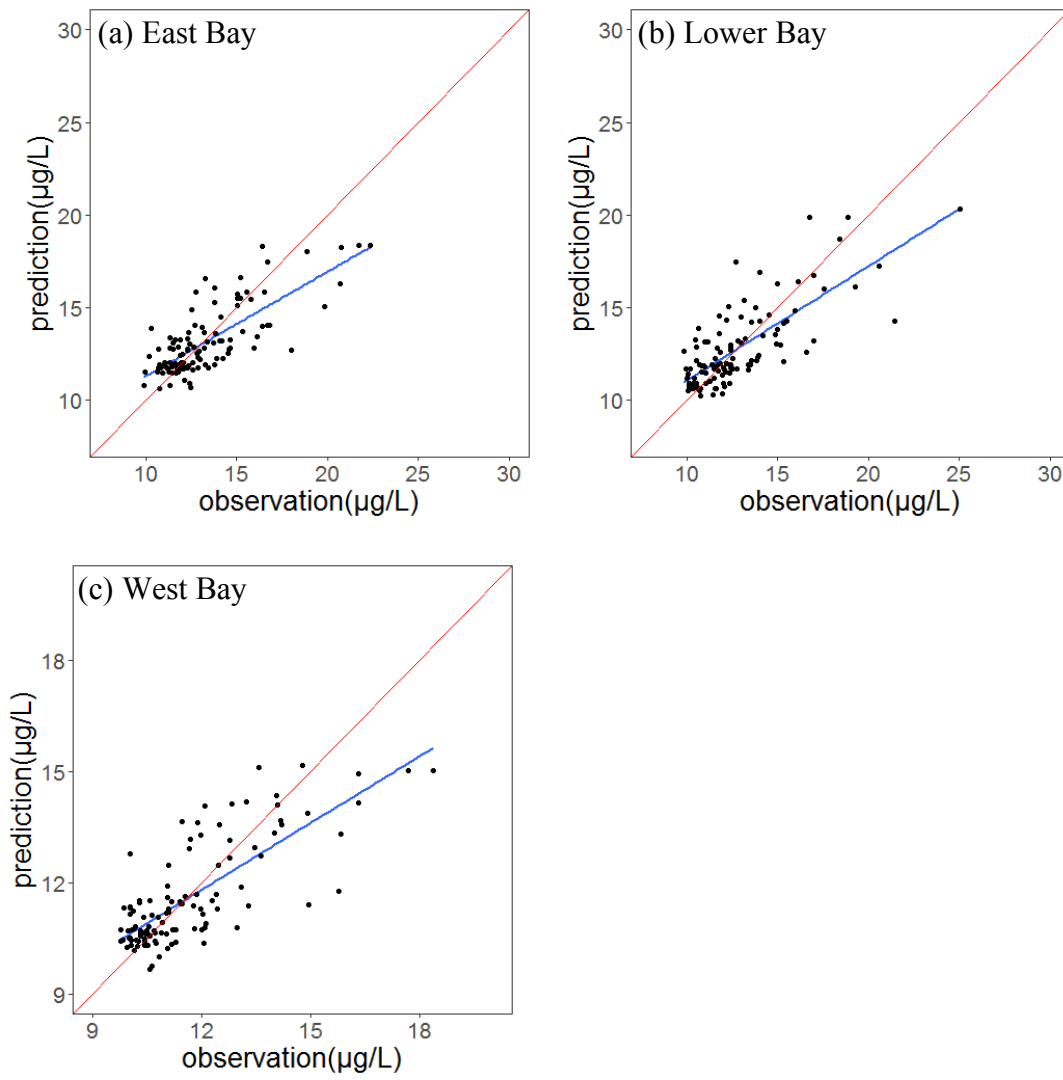


**Figure B-2** Comparison between prediction and observation chl a in (a) East Bay, (b) Lower Bay and (c) West Bay.